R. & M. No. 3029
(17,437)
A.R.C. Technical Report

MINISTRY OF SUPPLY

AERONAUTICAL RESEARCH COUNCIL
REPORTS AND MEMORANDA

Measurements of Two-Dimensional Derivatives on a Wing-Aileron-Tab System with a 1541 Section Aerofoil. Part II–Direct Tab and Cross Aileron-Tab Derivatives

By

K. C. WIGHT, A.F.R.Ae.S.,
of the Aerodynamics Division, N.P.L.

LONDON: HER MAJESTY'S STATIONERY OFFICE
1958
TEN SHILLINGS NET

Measurements of Two-Dimensional Derivatives on a Wing-Aileron-Tab System with a 1541 Section Aerofoil. Part II—Direct Tab and Cross Aileron-Tab Derivatives

By

K. C. WIGHT, A.F.R.Ae.S.
of the Aerodynamics Division, N.P.L.

Reports and Memoranda No. 3029
March, 1955

Summary.—Measurements have been made of the direct tab derivatives and cross aileron-tab derivatives for a 1541 section two-dimensional aerofoil (N.P.L. 282) with a 20 per cent aileron and 4 per cent (approx.) tab. In addition some measurements of the direct aileron derivatives have been made for comparison with earlier results together with a number of static derivatives for the wing and controls.

The influence is shown of frequency parameter, Reynolds number, position of transition, mean tab angle and sealing of the control hinge gaps. Some tests have been made with the aileron set at minus 8 deg and the tab at plus 12 deg for which condition the hinge moment on the aileron was zero.

Reasonable agreement with the values given by the ' equivalent profile ' theory is shown for both direct damping derivatives and for the direct tab stiffness derivative. The direct aileron stiffness derivative shows some departure from the theoretical value when $\omega > 1$.

At $\omega = 2$, $R = 10^6$ and the natural transition, comparison with the values given by flat-plate theory gives the following approximate factors, where suffix $_T$ denotes the theoretical values:

$$h_\beta/(h_\beta)_T = 0{\cdot}6,\ h_\gamma/(h_\gamma)_T = 0{\cdot}4,\ t_\beta/(t_\beta)_T = 0{\cdot}5,\ t_\gamma/(t_\gamma)_T = 0{\cdot}5$$
$$h_{\dot\beta}/(h_{\dot\beta})_T = 0{\cdot}6,\ h_{\dot\gamma}/(h_{\dot\gamma})_T = 0{\cdot}5,\ t_{\dot\beta}/(t_{\dot\beta})_T = 0{\cdot}5,\ t_{\dot\gamma}/(t_{\dot\gamma})_T = 0{\cdot}5.$$

1. *Introduction.*—The measurements described in this report continue the investigation described in an earlier report[1] to obtain a complete set of two-dimensional wing-aileron-tab derivatives using a 1541 section aerofoil (N.P.L. 282)[2] with a 20 per cent aileron and 4 per cent (approx.) tab.

The present report gives results obtained for the direct tab derivatives and cross aileron-tab derivatives. Some measurements of the direct aileron derivatives were also made for comparison with results given in Ref. 1 since a different tab was used. The trailing-edge angle of this tab was found to be different from that used in the earlier tests. Most tests were carried out with zero mean aileron angle, but a few measurements were made with the aileron set at 8 deg and the mean tab angle adjusted to give approximately zero hinge moment on the aileron. Mean tab settings of 0, 4 deg and 8 deg were used for measurements of the direct tab derivatives. Various corrections which have been applied to the experimental results are discussed in Appendix I.

Published with permission of the Director, National Physical Laboratory.

In addition to the oscillatory tests a comprehensive series of static tests was made to determine the values of the twelve stability derivatives a_n, b_n, c_n, m_n ($n = 1, 2, 3$). The effect of sealing the wing-aileron and aileron-tab gaps was also investigated. The results are given in Appendix II.

2. *Apparatus.*—A description of the apparatus used for the oscillatory measurements is given in Ref. 3, and details of the arrangement of the model in the tunnel and method of fixing transitions are given in Ref. 1.

A rolling axis at one end of the aerofoil and a pitching axis at the half-chord position were provided for the measurement of lift and pitching moment, but these freedoms were clamped for the oscillatory control tests. Use was made of these freedoms for the static tests. Balances attached at appropriate points allowed measurements to be made of the pitching moment and also of the moment about the rolling axis, from which the lift could be determined.

3. *Details of Model.*—

Section	1541 (N.P.L. 282)
Thickness/chord ratio ..	15 per cent
Trailing-edge angle	15 deg
Span	72 in.
Wing chord	30 in.
Aileron chord	6 in.
Tab chord	1·25 in.
Wing-aileron gap	0·06 in.
Aileron-tab gap	0·04 in.

Preliminary measurements of the direct tab derivatives made with the model described in Ref. 1 indicated that the torsional stiffness of the wooden tab was inadequate. For the present tests a new tab constructed of solid magnesium alloy was used. A theoretical estimate had shown that errors due to torsion should be negligible with this tab.

A diagram of the model is given in Fig. 1.

4. *Measurements.*—The direct tab derivatives were measured with the aileron locked to the wing and the aileron driving wires and quadrant removed. The latter were replaced for measurement of the forces on the aileron due to tab deflection and the aileron driving station was then disconnected from its eccentric. When it was required to measure the direct aileron derivatives, the aileron and tab were forced simultaneously with amplitudes which gave no movement of the tab relative to the aileron (*see* Appendix I, section 3) and the outputs from both aileron and tab electric balances were measured.

A frequency range from 3 c.p.s. to 12 c.p.s. was covered for each combination of Reynolds number and transition position with $\bar{\beta} = \bar{\gamma} = 0$. In the case of the tab, tests were also made with $\bar{\gamma} = 4$ deg and 8 deg. Some additional tests were made with $\bar{\beta} = -8$ deg and $\bar{\gamma} = +12{\cdot}4$ deg, which gave approximately zero aileron hinge moment in the mean position. All tests were made at Reynolds numbers of approximately 1, 2 and 3×10^6, and transition positions at $0{\cdot}1c$, $0{\cdot}4c$, and $0{\cdot}7c$ (natural) from the leading edge, except for the condition of $\bar{\beta} = -8$ deg, $\bar{\gamma} = +12{\cdot}4$ deg, where the transition position was fixed at $0{\cdot}1c$ only. The aileron and tab amplitudes were approximately 5 deg for all conditions tested.

5. *Tests with Control Gaps Sealed.*—The effect of sealing the wing-aileron gap was determined statically by applying across it a strip of tape 0·003 in. thick. Tests in which a tape was added to the surface without closing the gap showed appreciable aerodynamic interference. After

allowing for this effect it was found that the wing-aileron gap sealing produced a negligible effect on the static direct aileron derivatives. (A similar result is also indicated in Ref. 4, Fig. 14.) It was not possible to measure the effect with the control oscillating owing to the nature of the seal.

In the case of the aileron-tab gap, which was closed in the same way, both stiffness and damping for the direct aileron derivatives could be measured since the tab and aileron moved together. It was also possible to measure the cross tab derivatives due to aileron displacement.

Some measurements were made statically of the effect of sealing the aileron-tab gap on $-h_\gamma$ and $-t_\gamma$. Whilst there appeared to be little interference due to the tape it is thought that less reliance should be placed on these results than on those for $-h_\beta$ and $-t_\beta$ since the effective elastic stiffness of the seal was unknown. A knowledge of this was required since the correction for wing flexure for the static case depended on the bearing stiffness.

6. *Experimental Results.*—6.1. *Direct Tab Derivatives,* $-t_\gamma$, $-t_{\dot{\gamma}}$ (Figs. 2 to 5).—6.1.1. *Influence of frequency parameter.*—The stiffness derivative $-t_\gamma$ showed very little change over the ω-range for all conditions of the tests.

The damping derivative $-t_{\dot{\gamma}}$ showed little variation with frequency parameter for $\omega > 1{\cdot}5$. Below this value there was a falling off in damping which became more pronounced as the tab angle increased.

6.1.2. *Influence of Reynolds number.*—Scale effect on $-t_\gamma$ was small for all conditions tested. At the highest Reynolds number there was some increase in $-t_\gamma$ as ω increased. More marked effects were shown on the damping derivative $-t_{\dot{\gamma}}$, which in general, increased as the Reynolds number increased. This effect became less as the tab angle increased.

6.1.3. *Influence of tab angle.*—With the forward transition, increase of tab angle to 8 deg produced a rise of approximately 10 per cent in $-t_\gamma$, but there was little change with the natural transition.

Values of $-t_{\dot{\gamma}}$ increased by approximately 27 per cent as the tab angle was increased to 8 deg at the lowest speed and with forward transition. A slightly smaller increase was observed with the natural transition.

6.1.4. *Influence of transition position* (Figs. 12, 13).—Forward movement of transition reduced both $-t_\gamma$ and $-t_{\dot{\gamma}}$. When $\omega = 1{\cdot}2$, $\bar{\gamma} = 0$ and $R = 10^6$, this reduction amounted to 43 per cent for $-t_\gamma$ and 19 per cent for $-t_{\dot{\gamma}}$.

In the case of the stiffness derivative this change was similar for other values of ω and R. For the damping derivative below $\omega = 1$ the change was modified by scale effect and change of mean angle, the effect of change of transition position becoming less, in general, as the tab angle increased.

6.2. *Cross Derivatives for Tab Displacement,* $-h_\gamma$, $-h_{\dot{\gamma}}$ (Figs. 6, 7).—6.2.1. *Influence of frequency parameter.*—The tab cross stiffness and cross damping derivatives showed characteristics similar to the direct tab derivatives. The stiffness derivative $-h_\gamma$ showed little change with frequency parameter for the conditions tested, but the damping derivative $-h_{\dot{\gamma}}$ showed a rise above $\omega = 1{\cdot}5$, with a tendency to fall off as ω was decreased. This effect became less as the transition was moved forward.

6.2.2. *Influence of Reynolds number.*—Scale effect on $-h_\gamma$ was small, but $-h_{\dot{\gamma}}$ showed a rise as the Reynolds number was increased from 1 to 2×10^6, after which only minor changes occurred.

6.2.3. *Influence of transition position* (Figs. 12, 13).—Forward movement of transition reduced both $-h_\gamma$ and $-h_{\dot{\gamma}}$. When $\omega = 1{\cdot}2$, $\bar{\gamma} = 0$, and $R = 10^6$ this amounted to a reduction of 42 per cent for $-h_\gamma$ and 19 per cent for $-h_{\dot{\gamma}}$. The stiffness derivative showed similar changes for other values of ω and R, but for the damping derivative this reduction became less as the Reynolds number was increased.

6.3. *Direct Aileron Derivatives,* $-h_\beta$, $-h_{\dot{\beta}}$ (Figs. 8, 9).—Experimental results showing the influence on these derivatives of frequency parameter, Reynolds number, transition position, and mean aileron angle are reported in Ref. 1.

In the present tests, when the original wooden tab was replaced by a metal one, a difference in the direct aileron stiffness derivatives was observed for the two cases. After a number of possible sources of error had been examined it was found that the trailing-edge angle of the tab in the present case was larger than the previous one by $2\frac{1}{2}$ deg*. Values of $\partial C_H/\partial\beta$ measured for a range of trailing-edge angles are given in Refs. 5 and 6 and indicate that a difference in $-h_\beta$ could be expected due to this change of angle. From the charts given in Ref. 6 a reduction in $-h_\beta$ of 14 per cent with the forward transition and 7 per cent with the natural transition would be expected for an increase of $2\frac{1}{2}$ deg in trailing-edge angle. When these corrections are applied to the present measured values, they differ from those previously measured by about 5 per cent at $\omega = 0$ and less at higher values of ω.

The direct damping derivative $-h_{\dot{\beta}}$ showed only minor changes compared with the previously measured values, except for the condition of natural transition, where the scale effect was less marked.

The effect of sealing the aileron-tab gap (Fig. 14) was to increase the value of $-h_\beta$ by 14 per cent in the case of natural transition and 19 per cent for transition at $0{\cdot}1c$ when $\omega = 0$. Slightly smaller increases were observed at higher values of ω. The damping derivative $-h_{\dot{\beta}}$ showed an increase at $\omega = 1$ of about 11 per cent for both transition positions. The tests with sealed aileron-tab gap were made at $R = 10^6$ only.

6.4. *Cross Derivatives for Aileron Displacement,* $-t_\beta$, $-t_{\dot{\beta}}$ (Figs. 10, 11).—The influence of frequency parameter, Reynolds number, position of transition and a sealed gap was investigated.

The cross derivatives showed characteristics similar to those of the direct derivatives. The cross stiffness $-t_\beta$ varied approximately 40 per cent over the ω-range and was a minimum in the neighbourhood of $\omega = 0{\cdot}7$. Change of Reynolds number had little effect, although there was a tendency for $-t_\beta$ to rise at the highest speed. Change of transition from the natural position to $0{\cdot}1c$ produced a decrease of the order of 30 per cent. When the aileron-tab gap was sealed the value of the cross stiffness derivative increased for both transition positions and the whole ω-range to approximately double its value for the unsealed case.

The cross damping derivative $-t_{\dot{\beta}}$ showed little change with frequency parameter for $\omega > 1$. Below this value there was a falling off in damping. Change of Reynolds number from 2 to 3×10^6 produced an increase of the order of 15 per cent, but below this range there was little change. Change of transition position produced only minor changes in $-t_{\dot{\beta}}$. With the aileron-tab gap sealed the damping showed a rise of about 45 per cent over the ω-range used.

6.5. *Control Derivatives with Zero Hinge Moment* (Figs. 15, 16).—The influence of frequency parameter and Reynolds number was investigated and the tests were carried out with transition at $0{\cdot}1c$, $\bar{\beta} = -8$ deg and $\bar{\gamma} = +12{\cdot}4$ deg. All the stiffness derivatives showed a much increased scale effect, especially between Reynolds numbers of 1×10^6 and 2×10^6. In addition there was an increase in $-h_\beta$ of up to 16 per cent, depending on Reynolds number and an increase in $-t_\beta$ of about 100 per cent compared with the values for $\bar{\beta} = \bar{\gamma} = 0$.

The value of $-h_\gamma$ showed a decrease to about one half that obtained for $\bar{\beta} = \bar{\gamma} = 0$ and $-t_\gamma$ showed a decrease of from one half to one fifth depending on Reynolds number.

For the damping derivatives the scale effects were similar to those for zero mean control angles, except for $-t_{\dot{\beta}}$, which showed much larger effects. Changes in the magnitude of the damping derivatives tended to follow those in the stiffness derivatives but in the opposite sense. It was

* This may have been due to the surface finish applied to the wooden tab.

found that $-t_{\dot{\beta}}$ decreased to about half the value obtained with $\bar{\gamma} = \bar{\beta} = 0$, but $-h_{\dot{\beta}}$ showed little change. The increase in $-h_{\gamma}$, however, amounted to approximately 30 per cent with an increase in $-t_{\gamma}$ of up to about 25 per cent depending on Reynolds number.

7. *Comparison with Theory* (Figs. 17–19).—Since Part I of this report was published, C. S. Sinnott[7] (1953), has calculated values for the hinge moment derivatives for an oscillating control using the semi-empirical 'equivalent profile' theory suggested by W. P. Jones[8] (1948) which allows for aerofoil thickness and boundary-layer effects. Values for the direct aileron and tab derivatives have been calculated by this method using the experimentally determined values of a_2, b_2 and m_2, a_3, b_3 and m_3, given in this report. The results are plotted in Fig. 17. Reasonable agreement between these calculated values and those obtained from the oscillatory tests is shown for $-h_{\dot{\beta}}$, $-t_{\dot{\gamma}}$ and $-t_{\gamma}$ and also for $-h_{\beta}$ when $\omega < 1$. For $\omega > 1$, the experimental value of $-h_{\beta}$ increased with ω and with transition at $0{\cdot}4c$, $R = 10^6$ and $\omega = 3$, the difference amounted to approximately 25 per cent.

When the experimental results are compared with flat-plate theory[9] all the derivatives are found to be less by a factor of 0·4 to 0·6 (Figs. 18, 19). An increase in some of the derivatives as the frequency parameter is increased is also observed, which is not shown by flat-plate theory.

8. *Other Experimental Results.*—Andreopoulos, Cheilek and Donovan[10] (1949), who used a 40 per cent aileron and a 10 per cent tab obtained approximate agreement with flat-plate theory for the direct aileron derivatives. The direct tab stiffness $-t_{\gamma}$ was 0·75 to 0·8 of theory, whilst the tab damping $-t_{\dot{\gamma}}$ was 0·75 to 0·8 of theory for $\omega < 1{\cdot}3$. In the case of the cross derivatives, values of 0·7 of the theoretical were obtained for $-h_{\gamma}$ and 0·65 to 0·8 for $-t_{\beta}$. The value of $-h_{\dot{\gamma}}$ was 0·7 of theory, but that of $-t_{\dot{\beta}}$ only reached 0·7 of theory when ω approached 2.

Scruton, Raymer and Dunsdon[11] (1945) measured aerodynamic derivatives relating to wing-flexure aileron flutter for a B.A.C. Wing Type 167, of equivalent aspect ratio 9 (approx.) with a 20 per cent (approx.) control and obtained values of about 0·6 of flat-plate theory for the direct aileron derivatives.

NOTATION

H^*		Aileron hinge moment per unit span
	$=$	$\rho V^2 c^2\{(h_\beta + i\omega h_{\dot\beta} - \omega^2 h_{\ddot\beta})\beta + (h_\gamma + i\omega h_{\dot\gamma} - \omega^2 h_{\ddot\gamma})\gamma\}$
T		Tab hinge moment per unit span
	$=$	$\rho V^2 c^2[(t_\beta + i\omega t_{\dot\beta} - \omega^2 t_{\ddot\beta})\beta + (t_\gamma + i\omega t_{\dot\gamma} - \omega^2 t_{\ddot\gamma})\gamma]$
α		Angular displacement of aerofoil from mean position
β		Angular displacement of aileron from mean position
γ		Angular displacement of tab from mean position
β_o		Amplitude of oscillation of aileron
γ_o		Amplitude of oscillation of tab
$\bar\beta$		Mean aileron angle
$\bar\gamma$		Mean tab angle
ρ		Density
V		Wind speed
c		Aerofoil chord
R		Reynolds number
ν		Kinematic viscosity
f		Frequency
ω		Frequency parameter
	$=$	$\dfrac{2\pi fc}{V}$

$$a_1 = \frac{\partial C_L}{\partial \alpha}, \qquad a_2 = \frac{\partial C_L}{\partial \beta}, \qquad a_3 = \frac{\partial C_L}{\partial \gamma}$$

$$b_1 = \frac{\partial C_H}{\partial \alpha}, \qquad b_2 = \frac{\partial C_H}{\partial \beta}, \qquad b_3 = \frac{\partial C_H}{\partial \gamma}$$

$$c_1 = \frac{\partial C_{HT}}{\partial \alpha}, \qquad c_2 = \frac{\partial C_{HT}}{\partial \beta}, \qquad c_3 = \frac{\partial C_{HT}}{\partial \gamma}$$

$$m_1 = \frac{\partial C_m}{\partial \alpha}, \qquad m_2 = \frac{\partial C_m}{\partial \beta}, \qquad m_3 = \frac{\partial C_m}{\partial \gamma}$$

C_L	Lift coefficient
C_H	Aileron hinge-moment coefficient
C_{HT}	Tab hinge-moment coefficient
C_m	Pitching-moment coefficient referred to the half-chord axis

---

* The definition of H is in accordance with Ref. 9 but differs from that given in Part I of this report where the acceleration term was omitted.

REFERENCES

No.	*Author*	*Title, Etc.*
1	K. C. Wight	Measurements of two-dimensional derivatives on a wing-aileron-tab system with a 1541 section aerofoil. Part I. Direct aileron derivatives. R. & M. 2934. October, 1952.
2	R. C. Pankhurst	N.P.L. aerofoil catalogue and bibliography. C.P. 81. July, 1951. *See* also N.P.L. aerofoil sections; tabulated details. N.P.L./Aero/211. 1951.
3	J. B. Bratt and K. C. Wight	The effect of sweepback on the fundamental derivative coefficient for flexural motion. R. & M. 2774. October, 1950.
4	T. A. Toll	Summary of lateral control research. N.A.C.A. Tech. Note 1245. 1947.
5	L. E. Schneiter and R. L. Naeseth	Wind-tunnel investigation at low speeds of the lateral control characteristics of ailerons having three spans and three trailing-edge angles on a semi-span wing model. N.A.C.A. Tech. Note 1738. 1948.
6	L. W. Bryant, A. S. Halliday and A. S. Batson	Two-dimensional control characteristics. R. & M. 2730. April, 1950.
7	C. S. Sinnott	Hinge-moment derivatives for an oscillating control. Parts I and II. R. & M. 2923. September, 1953.
8	W. P. Jones	Aerofoil oscillations at high mean incidences. R. & M. 2654. April, 1948.
9	I. T. Minhinnick	Tables of functions for evaluation of wing and control-surface flutter derivatives for incompressible flow. R.A.E. Report Structures 86. A.R.C. 13,730. July, 1950.
10	T. C. Andreopoulos, H. A. Cheilek and A. F. Donovan.	Measurements of the aerodynamic hinge moments of an oscillating flap and tab. U.S.A.F. Tech. Report 5784. 1949.
11	C. Scruton, W. G. Raymer and Miss D. V. Dunsdon.	Experimental determination of the aerodynamic derivatives for flexural-aileron flutter of B.A.C. Wing type 167. R. & M. 2373. May, 1945.
12	W. P. Jones	Wind-tunnel interference effect on the value of experimentally determined derivative coefficients for oscillating aerofoils. R. & M. 1912. August, 1943.
13	W. P. Jones	Wind-tunnel interference effects on measurements of aerodynamic coefficients for oscillating aerofoils. R. & M. 2786. September, 1950.
14	E. Reissner	Wind-tunnel corrections for the two-dimensional theory of oscillating airfoils. Report SB-318-S-3. Cornell Aero. Lab. Inc. 1947.
15	E. M. de Jager	The aerodynamic forces and moments on an oscillating aerofoil with control surface between two parallel walls. N.L.L. Report F.140. 1953.

APPENDIX I

Corrections.—During the tests the model distorted in several ways. Some of these produced appreciable errors for which corrections had to be made. In addition, certain corrections for amplitude and phase, apparatus damping and parasitic moments have been applied. These, together with a reference to tunnel interference, are described below under separate headings.

1. *Tunnel Interference.*—The effect of tunnel-wall interference on derivative coefficients for oscillating models has been investigated by W. P. Jones[12, 13] (1943, 1950), Reissner[14] (1947), Sinnott[7] (1953) and de Jager[15] (1953). A comparison between the results of Sinnott (equivalent profile) and those of de Jager (hinged plate) for a 20 per cent control, where the wing chord/tunnel height ratio was 0·35 (approx.) is shown in Fig. 20. The correction due to interference amounts to a maximum of about 7 per cent for both damping and stiffness derivatives in the region of $\omega = 0{\cdot}5$, and decreases to about 2 per cent or less for $\omega > 1$.

No corrections have been applied to the oscillatory derivatives for this effect nor for the effect of tunnel blockage. The static blockage amounted to $\Delta V/V = 1{\cdot}3$ per cent for the highest speed.

2. *Distortion of Model.*—Reference has already been made in an earlier report[1] to the flexure of the wing due to the oscillatory air-loads, which produced an error in the measured aileron forces through inertial coupling. A semi-empirical method of correcting for this error was devised. In the present case preliminary measurements of the direct tab stiffness derivatives were found to be in error both due to wing flexure and to ' blowback ' of the driving wires. The latter produced not only a movement of the control but a reduction in the effective stiffness of the driving member. This effect had been smaller in the tests of Ref. 1, on account of the greater tensions employed, and was corrected by the method described in that report.

Since attempts to allow for the ' blowback ' effects were unsatisfactory in the present case, the driving wires were finally shielded with streamlined guards. Tests in which additional guards were placed in the tunnel indicated that aerodynamic interference was negligible.

Errors due to wing flexure were then calculated from measurements of the vertical translation at the section containing the driving quadrant and the product of inertia between this motion and the tab or aileron freedom. Measurements of both amplitude and phase of the vertical translation relative to the control-surface motion were made, and the appropriate component of the inertial reaction was used in determining the corrections for both stiffness and damping derivatives. Those for the latter were small (< 2 per cent for $\omega > 0{\cdot}5$, rising to 6 per cent at $\omega = 0{\cdot}2$) and since small phase angles were involved which were difficult to measure accurately, the corrections have not been applied in the case of the damping.

Errors in the direct tab and aileron derivatives due to twist of the control were estimated by calculations involving β or γ and the twist. An expression for the error was derived in a form involving torsional stiffness and inertia, the direct hinge-moment derivative and mode of twist. Measured values of these quantities were substituted with the exception of the mode, which was assumed to be the same as that calculated for the still-air case. The error was negligible for the tab stiffness derivative and about 2 per cent for the damping derivative, whilst for the aileron it was negligible for the damping and about 4 per cent for the stiffness derivative. However, optical measurements indicated that the twist and hence the errors were smaller than calculated and for this reason no corrections were applied.

3. *Amplitude and Phase Measurements.*—The forced amplitude of the controls was found to increase slightly with frequency due to flexibility in the forcing linkage. To allow for this the amplitude was measured optically at each frequency.

For mechanical reasons it was not possible to set the amplitude and phase of tab and aileron motions to give exactly zero movement of the tab relative to the aileron. Thus in the determination of $-h_\beta$, $-h_{\dot\beta}$, $-t_\beta$ and $-t_{\dot\beta}$ it was necessary to measure both the amplitude and phase of the motions optically to enable small corrections to be applied using the previously measured values of $-h_\gamma$, $-h_{\dot\gamma}$, $-t_\gamma$, $-t_{\dot\gamma}$.

4. *Apparatus Damping.*—Corrections to the derivatives $-h_{\dot\beta}$ and $-t_{\dot\beta}$ for apparatus damping were measured in the manner described in Ref. 1. In estimating the apparatus damping relating to $-h_{\dot\gamma}$, the still-air damping was assumed to be negligible. In the case of the derivative $-t_{\dot\gamma}$, attempts to separate the apparatus and still-air damping failed because the apparatus hysteresis was large compared with the still-air damping. It was possible, however, to estimate the order of magnitude of the still-air damping for the tab from that measured on the aileron. It may be shown by dimensional theory that the damping coefficient per unit span is of the form $\rho c^4 f \phi(c^2 f/v)$, where $\phi(c^2 f/v)$ is some function of $(c^2 f/v)$. The aileron tests indicated a constant magnitude for $\phi(c^2 f/v)$ for the higher values of $(c^2 f/v)$, with a falling off in magnitude as values of $(c^2 f/v)$, appropriate to the tab were approached. Calculations of the tab still-air damping based on the constant value of $\phi(c^2 f/v)$ gave over-estimated values which were found to be negligible in comparison with the aerodynamic damping.

5. *Miscellaneous Corrections.*—The effect of forces on the sting bearings and quadrants was determined by the addition of dummy bearings and quadrants, which in the case of the tab moved with the control. Allowance had to be made for the change in the product of inertia of the system in estimating errors due to wing flexure. In the case of the aileron the measurements were made statically because of the large inertia involved and the difficulty of estimating the change in the product of inertia accurately. The effect of drag moment due to the exposed portions of the driving wires was calculated from wire drag measurements.

APPENDIX II

Measurement of Static-Wing and Control Derivatives

A knowledge of the wing static-stability derivatives is necessary for the calculation of the oscillatory control derivatives by the ' equivalent profile ' method. These, together with the control derivatives provide additional information for the two-dimensional stability and control programme. Hence static measurements have been made of the lift and pitching moment on the aerofoil due to change of α, β and γ. In addition, static hinge moments on the controls have been measured for a range of control settings. In the case of the lift and pitching moments a Reynolds number of 10^6 was chosen, since wing distortion was likely to be least for this value, but for the control hinge moments a value of 2×10^6 was used, since increased accuracy would be obtained.

The stability derivatives tabulated have been obtained from curves of lift, pitching moment and hinge moment and correspond to the slope at the origin, after allowing for tunnel blockage and wall interference.

Least reliance should be placed on the values of c_1, c_2 and c_3 obtained with the aileron-tab gap sealed, since the sealing, as mentioned in section 5 may have produced other effects, besides preventing the flow through the gap.

Tabulated Results : Flutter Derivatives

Transition at $0 \cdot 1c$

TABLE 1—$R = 10^6$

	$\bar{\gamma} = 0$ deg		$\bar{\gamma} = 4$ deg		$\bar{\gamma} = 8$ deg	
ω	$-t_\gamma \times 10^4$	$-t_\dot{\gamma} \times 10^5$	$-t_\gamma \times 10^4$	$-t_\dot{\gamma} \times 10^5$	$-t_\gamma \times 10^4$	$-t_\dot{\gamma} \times 10^5$
0	2·28	—	2·40	—	2·46	—
0·73	2·28	—	2·35	—	2·38	—
1·21	2·29	3·13	2·41	3·36	2·44	4·30
1·69	2·30	3·13	2·35	3·39	2·46	4·30
2·17	2·30	3·19	2·33	3·49	2·51	4·20
2·66	2·31	3·43	2·38	3·51	2·47	4·13
2·90	2·32	3·49	2·35	3·47	2·53	4·13

TABLE 2—$R = 2 \times 10^6$

	$\bar{\gamma} = 0$ deg		$\bar{\gamma} = 4$ deg		$\bar{\gamma} = 8$ deg	
ω	$-t_\gamma \times 10^4$	$-t_\dot{\gamma} \times 10^5$	$-t_\gamma \times 10^4$	$-t_\dot{\gamma} \times 10^5$	$-t_\gamma \times 10^4$	$-t_\dot{\gamma} \times 10^5$
0	2·20	—	2·37	—	2·49	—
0·36	2·32	—	2·36	—	2·52	—
0·60	2·32	3·52	2·38	3·34	2·54	3·70
0·85	2·26	3·61	2·36	3·56	2·56	4·03
1·09	2·25	3·75	2·39	3·71	2·56	4·22
1·33	2·29	3·84	2·40	3·79	2·59	4·35
1·45	2·27	3·88	2·39	3·75	2·58	4·37

TABLE 3—$R = 3 \times 10^6$

	$\bar{\gamma} = 0$ deg		$\bar{\gamma} = 4$ deg		$\bar{\gamma} = 8$ deg	
ω	$-t_\gamma \times 10^4$	$-t_\dot{\gamma} \times 10^5$	$-t_\gamma \times 10^4$	$-t_\dot{\gamma} \times 10_5$	$-t_\gamma \times 10^4$	$-t_\dot{\gamma} \times 10^5$
0	2·28	—	2·42	—	2·44	—
0·23	2·29	—	2·38	—	2·46	—
0·38	2·30	3·35	2·39	3·23	2·51	3·23
0·53	2·31	3·55	2·43	3·44	2·57	3·63
0·69	2·32	3·68	2·42	3·65	2·61	3·92
0·84	2·35	3·78	2·52	3·79	2·71	4·13
0·92	2·36	3·84	2·59	3·85	2·73	4·18

Transition at 0·4*c*

TABLE 4—$\bar{\gamma} = 0$ deg

$R = 10^6$			$R = 2\times10^6$			$R = 3\times10^6$		
ω	$-t_\gamma\times10^4$	$-t_{\dot\gamma}\times10^5$	ω	$-t_\gamma\times10^4$	$-t_{\dot\gamma}\times10^5$	ω	$-t_\gamma\times10^4$	$-t_{\dot\gamma}\times10^5$
0	2·93	—	0	2·90	—	0	2·90	—
0·73	2·93	—	0·36	2·91	—	0·23	2·90	—
1·21	2·90	3·56	0·60	2·88	3·39	0·38	2·90	3·22
1·69	2·87	3·71	0·85	2·89	3·75	0·53	2·92	3·65
2·17	2·87	3·69	1·09	2·87	3·94	0·69	2·93	3·87
2·66	2·87	3·59	1·33	2·88	3·96	0·84	2·95	3·99
2·90	2·87	3·49	1·45	2·88	3·99	0·92	2·98	4·03

Natural Transition

TABLE 5—$R = 10^6$

	$\bar{\gamma} = 0$ deg		$\bar{\gamma} = 4$ deg		$\bar{\gamma} = 8$ deg	
ω	$-t_\gamma\times10^4$	$-t_{\dot\gamma}\times10^5$	$-t_\gamma\times10^4$	$-t_{\dot\gamma}\times10^5$	$-t_\gamma\times10^4$	$-t_{\dot\gamma}\times10^5$
0	4·16	—	4·06	—	4·00	—
0·73	4·01	—	3·92	—	3·79	—
1·21	3·97	3·89	3·89	4·96	3·81	4·62
1·69	3·99	3·93	3·93	4·99	3·87	5·07
2·17	4·05	4·15	3·97	4·97	3·93	5·12
2·66	4·10	4·46	4·07	4·83	4·05	5·11
2·90	4·30	4·67	4·12	4·67	4·15	5·01

TABLE 6—$R = 2 \times 10^6$

	$\bar{\gamma} = 0$ deg		$\bar{\gamma} = 4$ deg		$\bar{\gamma} = 8$ deg	
ω	$-t_\gamma\times10^4$	$-t_{\dot\gamma}\times10^5$	$\times t_\gamma\times10^4$	$-t_{\dot\gamma}\times10^5$	$-t_\gamma\times10^4$	$-t_{\dot\gamma}\times10^5$
0	3·83	—	3·96	—	3·81	—
0·36	3·87	—	4·03	—	3·84	—
0·60	3·96	4·13	4·08	3·59	3·97	3·76
0·85	3·96	4·33	4·15	4·12	3·98	4·54
1·09	3·95	4·56	4·16	4·39	4·00	4·99
1·33	3·93	4·76	4·11	4·48	4·03	5·27
1·45	4·03	4·85	4·08	4·50	4·06	5·38

Natural Transition

TABLE 7—$R = 3 \times 10^6$

	$\bar{\gamma} = 0$ deg		$\bar{\gamma} = 4$ deg		$\gamma = 8$ deg	
ω	$-t_\gamma \times 10^4$	$-t_{\bar{\gamma}} \times 10^5$	$-t_\gamma \times 10^4$	$-t_{\bar{\gamma}} \times 10^5$	$-t_\gamma \times 10^4$	$-t_{\bar{\gamma}} \times 10^5$
0	3·69	—	3·79	—	3·60	—
0·23	3·80	—	3·90	—	3·88	—
0·38	3·84	4·15	3·94	3·04	3·98	2·72
0·53	3·94	4·36	4·02	3·57	4·05	3·44
0·69	3·95	4·47	4·06	3·75	4·10	3·79
0·84	3·96	4·52	4·13	3·88	4·09	4·13
0·92	3·99	4·54	4·13	3·93	4·08	4·29

Transition at 0·1*c*

TABLE 8—$\bar{\gamma} = 0$ deg

$R = 10^6$			$R = 2 \times 10^6$			$R = 3 \times 10^6$		
ω	$-h_\gamma \times 10^2$	$-h_{\bar{\gamma}} \times 10^3$	ω	$-h_\gamma \times 10^2$	$-h_{\bar{\gamma}} \times 10^3$	ω	$-h_\gamma \times 10^2$	$-h_{\bar{\gamma}} \times 10^3$
0	0·615	—	0	0·620	—	0	0·635	—
0·73	0·595	0·275	0·36	0·600	0·275	0·23	0·615	0·210
1·21	0·605	0·475	0·60	0·600	0·445	0·38	0·610	0·305
1·69	0·595	0·535	0·85	0·595	0·520	0·53	0·610	0·405
2·17	0·600	0·565	1·09	0·590	0·574	0·69	0·610	0·470
2·66	0·600	0·585	1·33	0·595	0·600	0·84	0·610	0·505
2·90	0·595	0·595	1·45	0·595	0·613	0·92	0·610	0·520

Transition at 0·4*c*

TABLE 9—$\bar{\gamma} = 0$ deg

$R = 10^6$			$R = 2 \times 10^6$			$R = 3 \times 10^6$		
ω	$-h_\gamma \times 10^2$	$-h_{\bar{\gamma}} \times 10^3$	ω	$-h_\gamma \times 10^2$	$-h_{\bar{\gamma}} \times 10^3$	ω	$-h_\gamma \times 10^2$	$-h_{\bar{\gamma}} \times 10^3$
0	0·795	—	0	0·780	—	0	0·795	—
0·73	0·760	0·425	0·36	0·755	0·240	0·23	0·780	0·285
1·21	0·755	0·525	0·60	0·750	0·400	0·38	0·775	0·485
1·69	0·755	0·560	0·85	0·745	0·495	0·53	0·755	0·585
2·17	0·755	0·600	1·09	0·740	0·575	0·69	0·755	0·650
2·66	0·755	0·635	1·33	0·745	0·635	0·84	0·770	0·700
2·90	0·750	0·650	1·45	0·745	0·665	0·91	0·771	0·725

Natural Transition

TABLE 10—$\bar{\gamma} = 0$ deg

$R = 10^6$			$R = 2\times10^6$			$R = 3\times10^6$		
ω	$-h_\gamma\times10^2$	$-h_{\dot\gamma}\times10^3$	ω	$-h_\gamma\times10^2$	$-h_{\dot\gamma}\times10^3$	ω	$-h_\gamma\times10^2$	$-h_{\dot\gamma}\times10^3$
0	1·07	—	0	1·05	—	0	1·02	—
0·73	1·04	0·530	0·36	1·02	0·285	0·23	1·01	0·145
1·21	1·04	0·585	0·60	1·02	0·485	0·38	1·01	0·305
1·69	1·04	0·640	0·85	1·01	0·585	0·53	1·02	0·415
2·17	1·05	0·685	1·09	1·02	0·650	0·69	1·02	0·485
2·66	1·06	0·725	1·33	1·03	0·700	0·84	1·03	0·530
2·90	1·07	0·745	1·45	1·03	0·725	0·91	1·02	0·545

Transition at 0·1*c*

TABLE 11—$\bar{\beta} = 0$ deg

$R = 10^6$			$R = 2\times10^6$			$R = 3\times10^6$		
ω	$-h_\beta\times10^2$	$-h_{\dot\beta}\times10^2$	ω	$-h_\beta\times10^2$	$-h_{\dot\beta}\times10^2$	ω	$-h_\beta\times10^2$	$-h_{\dot\beta}\times10^2$
0	0·765	—	0	0·775	—	0	0·810	—
0·73	0·725	0·390	0·36	0·740	0·365	0·23	0·785	0·360
1·21	0·785	0·425	0·60	0·720	0·400	0·38	0·765	0·385
1·69	0·770	0·430	0·85	0·725	0·430	0·53	0·755	0·425
2·17	0·800	0·455	1·09	0·730	0·455	0·69	0·750	0·460
2·66	0·855	0·470	1·33	0·755	0·470	0·84	0·760	0·475
2·90	0·875	0·480	1·45	0·750	0·480	0·91	0·765	0·485

Transition at 0·4*c*

TABLE 12—$\bar{\beta} = 0$ deg

$R = 10^6$			$R = 2\times10^6$			$R = 3\times10^6$		
ω	$-h_\beta\times10^2$	$-h_{\dot\beta}\times10^2$	ω	$-h_\beta\times10^2$	$-h_{\dot\beta}\times10^2$	ω	$-h_\beta\times10^2$	$-h_{\dot\beta}\times10^2$
0	0·91	—	0	0·98	—	0	0·92	—
0·73	0·83	0·400	0·36	0·83	0·305	0·23	0·88	0·315
1·21	0·83	0·425	0·60	0·81	0·395	0·38	0·86	0·365
1·69	0·86	0·445	0·85	0·81	0·435	0·53	0·85	0·410
2·17	0·91	0·470	1·09	0·82	0·465	0·69	0·84	0·450
2·66	0·96	0·480	1·33	0·84	0·485	0·84	0·84	0·475
2·90	1·01	0·485	1·45	0·84	0·495	0·91	0·85	0·485

(68305)

Natural Transition

TABLE 13—$\bar{\beta} = 0$ deg

$R = 10^6$			$R = 2\times10^6$			$R = 3\times10^6$		
ω	$-h_\beta\times10^2$	$-h_{\dot\beta}\times10^2$	ω	$-h_\beta\times10^2$	$-h_{\dot\beta}\times10^2$	ω	$-h_\beta\times10^2$	$-h_{\dot\beta}\times10^2$
0	1·08	—	0	1·05	—	0	1·04	—
0·73	0·99	0·405	0·36	0·99	0·335	0·23	1·02	0·350
1·21	1·03	0·470	0·60	0·97	0·405	0·38	1·01	0·390
1·69	0·99	0·480	0·85	0·94	0·445	0·53	1·00	0·420
2·17	1·01	0·510	1·09	0·96	0·475	0·69	0·99	0·450
2·66	1·04	0·525	1·33	1·01	0·500	0·84	1·00	0·480
2·90	1·04	0·540	1·45	0·98	0·515	0·91	1·00	0·485

Transition at 0·1c

TABLE 14—$\bar{\beta} = 0$ deg

$R = 10^6$			$R = 2\times10^6$			$R = 3\times10^6$		
ω	$-t_\beta\times10^4$	$-t_{\dot\beta}\times10^4$	ω	$-t_\beta\times10^4$	$-t_{\dot\beta}\times10^4$	ω	$-t_\beta\times10^4$	$-t_{\dot\beta}\times10^4$
0	1·05	—	0	1·04	—	0	1·16	—
0·73	0·82	1·01	0·36	0·96	0·92	0·23	1·08	0·83
1·21	1·26	0·88	0·60	0·84	0·98	0·38	1·05	0·99
1·69	1·24	0·82	0·85	1·00	0·99	0·53	1·08	1·06
2·17	1·43	0·80	1·09	1·09	1·01	0·69	1·15	1·10
2·66	1·12	0·80	1·33	1·17	1·02	0·84	1·15	1·12
2·90	1·34	0·80	1·45	1·02	1·03	0·91	1·17	1·13

Transition at 0·4c

TABLE 15—$\bar{\beta} = 0$ deg

$R = 10^6$			$R = 2\times10^6$			$R = 3\times10^6$		
ω	$-t_\beta\times10^4$	$-t_{\dot\beta}\times10^4$	ω	$-t_\beta\times10^4$	$-t_{\dot\beta}\times10^4$	ω	$-t_\beta\times10^4$	$-t_{\dot\beta}\times10^4$
0	1·43	—	0	1·09	—	0	1·29	—
0·73	1·25	0·88	0·36	0·99	0·89	0·23	1·14	0·73
1·21	1·06	0·91	0·60	0·91	1·00	0·38	1·09	0·97
1·69	1·25	0·92	0·85	0·97	1·04	0·53	1·09	1·07
2·17	1·73	0·96	1·09	1·01	1·08	0·69	1·11	1·13
2·66	1·71	0·95	1·33	1·09	1·09	0·84	1·15	1·16
2·90	1·82	0·98	1·45	1·24	1·11	0·91	1·22	1·18

Natural Transition

TABLE 16—$\bar{\beta} = 0$ deg

$R = 10^6$			$R = 2\times10^6$			$R = 3\times10^6$		
ω	$-t_\beta\times10^4$	$-t_{\dot\beta}\times10^4$	ω	$-t_\beta\times10^4$	$-t_{\dot\beta}\times10^4$	ω	$-t_\beta\times10^4$	$-t_{\dot\beta}\times10^4$
0	1·40	—	0	1·28	—	0	1·31	—
0·73	1·49	1·03	0·36	1·12	0·77	0·23	1·30	1·08
1·21	1·37	1·00	0·60	1·18	0·95	0·38	1·31	1·11
1·69	1·37	0·99	0·85	1·29	1·03	0·53	1·34	1·13
2·17	1·50	1·01	1·09	1·32	1·08	0·69	1·34	1·14
2·66	1·52	1·00	1·33	1·32	1·11	0·84	1·43	1·14
2·90	1·56	1·04	1·45	1·25	1·12	0·91	1·39	1·15

Transition at 0·1*c*

TABLE 17—$\bar{\beta} = -8$ deg, $\bar{\gamma} = +12{\cdot}4$ deg

$R = 10^6$			$R = 2\times10^6$			$R = 3\times10^6$		
ω	$-t_\gamma\times10^4$	$-t_{\dot\gamma}\times10^5$	ω	$-t_\gamma\times10^4$	$-t_{\dot\gamma}\times10^5$	ω	$-t_\gamma\times10^4$	$-t_{\dot\gamma}\times10^5$
0	1·63	—	0	0·98	—	0	0·92	—
0·73	1·43	—	0·36	1·02	—	0·23	0·94	—
1·21	1·41	3·30	0·60	0·97	4·74	0·38	0·91	3·90
1·69	1·38	3·47	0·85	0·93	4·83	0·53	0·90	4·14
2·17	1·37	3·79	1·09	0·93	4·82	0·69	0·89	4·41
2·66	1·37	3·79	1·33	0·96	4·86	0·84	0·90	4·78
2·90	1·38	4·35	1·45	0·99	4·85	0·91	0·91	4·91

TABLE 18

$R = 10^6$			$R = 2\times10^6$			$R = 3\times10^6$		
ω	$-h_\gamma\times10^2$	$-h_{\dot\gamma}\times10^3$	ω	$-h_\gamma\times10^2$	$-h_{\dot\gamma}\times10^3$	ω	$-h_\gamma\times10^2$	$-h_{\dot\gamma}\times10^3$
0	0·336	—	0	0·292	—	0	0·296	—
0·73	0·332	0·645	0·36	0·295	0·685	0·23	0·297	0·565
1·21	0·324	0·720	0·60	0·289	0·720	0·38	0·295	0·605
1·69	0·326	0·760	0·85	0·286	0·745	0·53	0·288	0·675
2·17	0·322	0·795	1·09	0·281	0·795	0·69	0·286	0·710
2·66	0·326	0·825	1·33	0·278	0·830	0·84	0·282	0·755
2·90	0·333	0·830	1·45	0·276	0·840	0·91	0·283	0·780

Transition at 0·1*c*

TABLE 19—$\bar{\beta} = -8$ deg, $\bar{\gamma} = +12{\cdot}4$ deg

$R = 10^6$			$R = 2\times10^6$			$R = 3\times10^6$		
ω	$-h_\beta\times10^2$	$-h_{\hat{\beta}}\times10^2$	ω	$-h_\beta\times10^2$	$-h_{\hat{\beta}}\times10^2$	ω	$-h_\beta\times10^2$	$-h_{\hat{\beta}}\times10^2$
0	0·815	—	0	0·860	—	0	0·910	—
0·73	0·795	0·405	0·36	0·835	0·425	0·23	0·875	0·435
1·21	0·810	0·400	0·60	0·835	0·440	0·38	0·875	0·450
1·69	0·845	0·400	0·85	0·855	0·435	0·53	0·875	0·460
2·17	0·880	0·400	1·09	0·870	0·440	0·69	0·880	0·465
2·66	0·935	0·405	1·33	0·895	0·445	0·84	0·890	0·475
2·90	0·965	0·405	1·45	0·905	0·450	0·91	0·895	0·480

TABLE 20

$R = 10^6$			$R = 2\times10^6$			$R = 3\times10^6$		
ω	$-t_\beta\times10^4$	$-t_{\hat{\beta}}\times10^5$	ω	$-t_\beta\times10^4$	$-t_{\hat{\beta}}\times10^5$	ω	$-t_\beta\times10^4$	$-t_{\hat{\beta}}\times10^5$
0	1·87	—	0	1·80	—	0	1·92	—
0·73	1·58	5·01	0·36	1·82	5·13	0·23	1·89	3·89
1·21	1·44	3·78	0·60	1·75	4·84	0·38	1·94	5·01
1·69	1·69	3·31	0·85	1·85	4·83	0·53	1·96	5·57
2·17	1·59	3·27	1·09	2·02	4·92	0·69	2·07	5·80
2·66	1·98	3·31	1·33	1·97	4·99	0·84	2·09	6·02
2·90	2·06	3·28	1·45	2·01	5·01	0·91	2·09	6·06

Tabulated Results : Stability Derivatives

TABLE 21—$R = 10^6$

Transition	Aileron-tab gap	a_1	m_1	a_2	$-m_2$	a_3	$-m_3$
0·1c	Open	4·73	$0·00_5$	1·92	$0·36_5$	0·44	0·103
0·4c	Open	5·06	$0·02_5$	2·16	$0·41_5$	—	—
Natural	Open	5·16	0·07	2·42	$0·47_5$	0·70	0·169
0·1c	Sealed	4·92	$0·02_5$	2·09	0·41	0·635	0·147
0·4c	Sealed	5·16	0·07	2·31	$0·45_5$	—	—
Natural	Sealed	5·27	$0·09_5$	2·58	0·51	0·91	0·213

TABLE 22—$R = 2 \times 10^6$

Transition	Aileron-tab gap	$-b_1$	$-c_1$	$-b_2$	$-c_2$	$-b_3$	$-c_3$
0·1c	Open	0·06	$0·05_5$	0·36	0·08	$0·27_5$	0·22
0·4c	Open	—	—	0·42	0·09	0·38	0·29
Natural	Open ($R = 10^6$)	(0·14) 0·12	0·07	$0·49_5$	$0·09_5$	0·48	0·43
0·1c	Sealed	0·11	—	$0·45_5$	$0·19_5$	—	—
0·4c	Sealed	—	—	$0·51_5$	0·28	0·57	0·49
Natural	Sealed	0·16	0·03	0·56	$0·29_5$	—	—

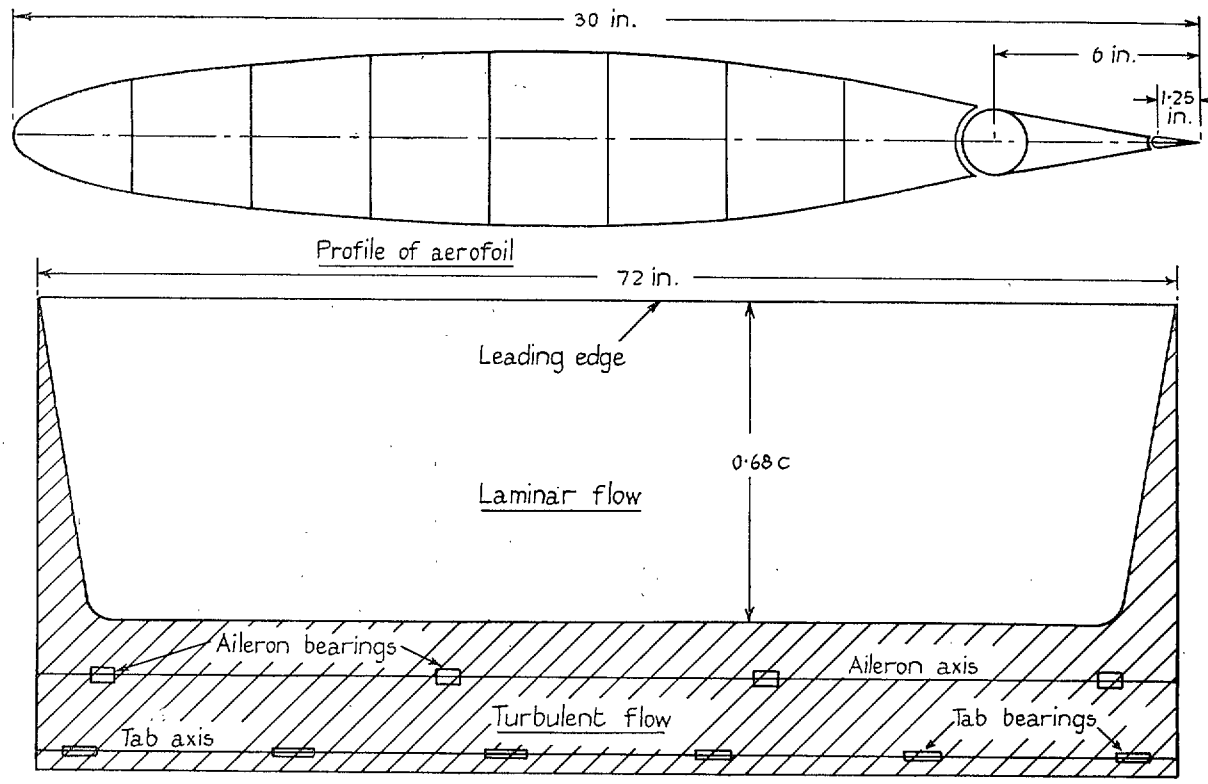

FIG. 1. Plan of aerofoil showing natural transition at $R = 0{\cdot}94 \times 10^6$.

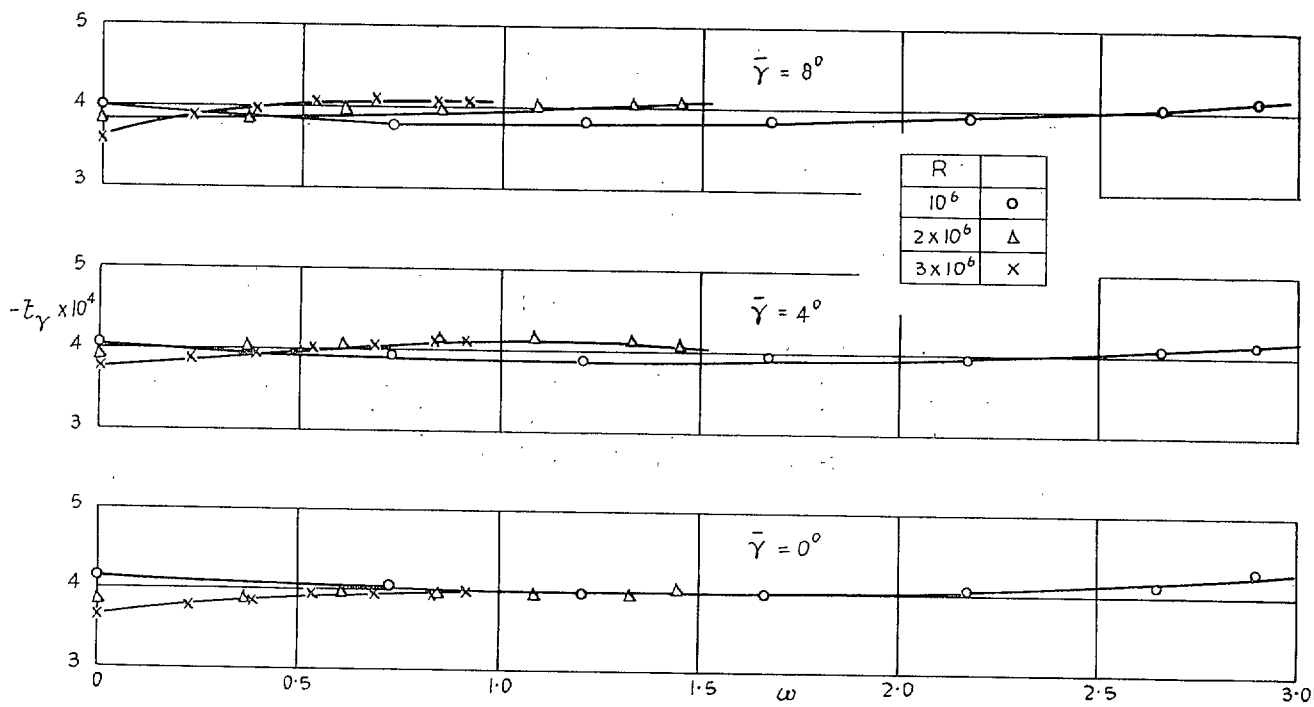

FIG. 2. Variation of t_γ with frequency parameter—natural transition.

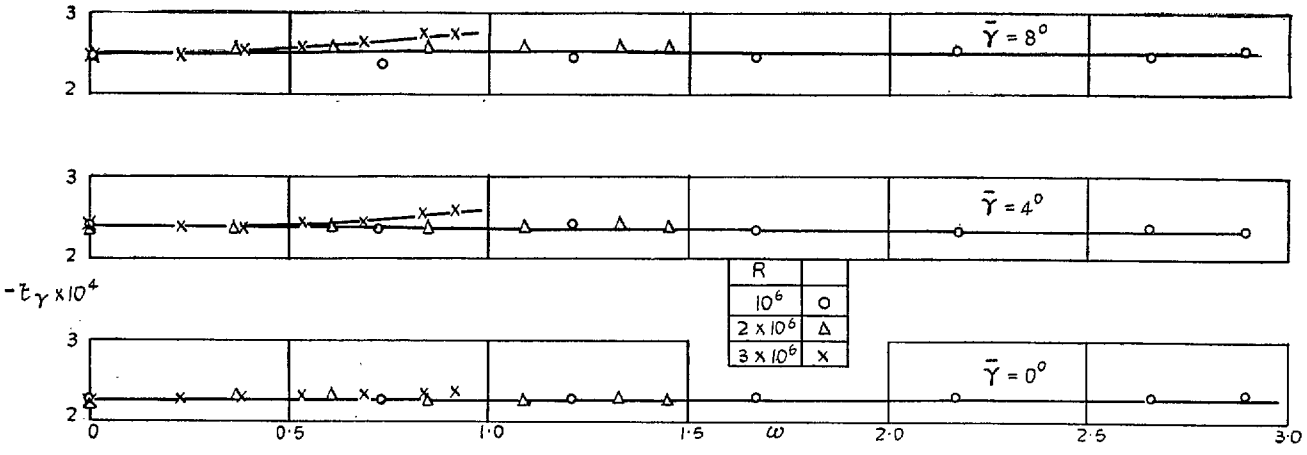

Variation of t_γ with frequency parameter—transition at 0·1c.

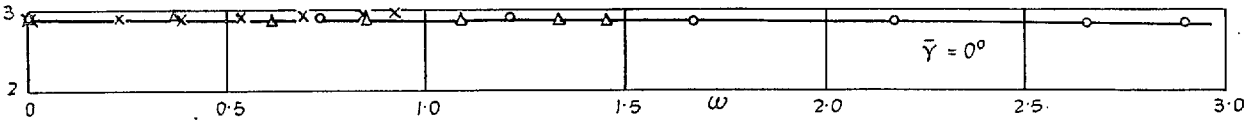

FIG. 3. Variation of t_γ with frequency parameter— transition at 0·4c.

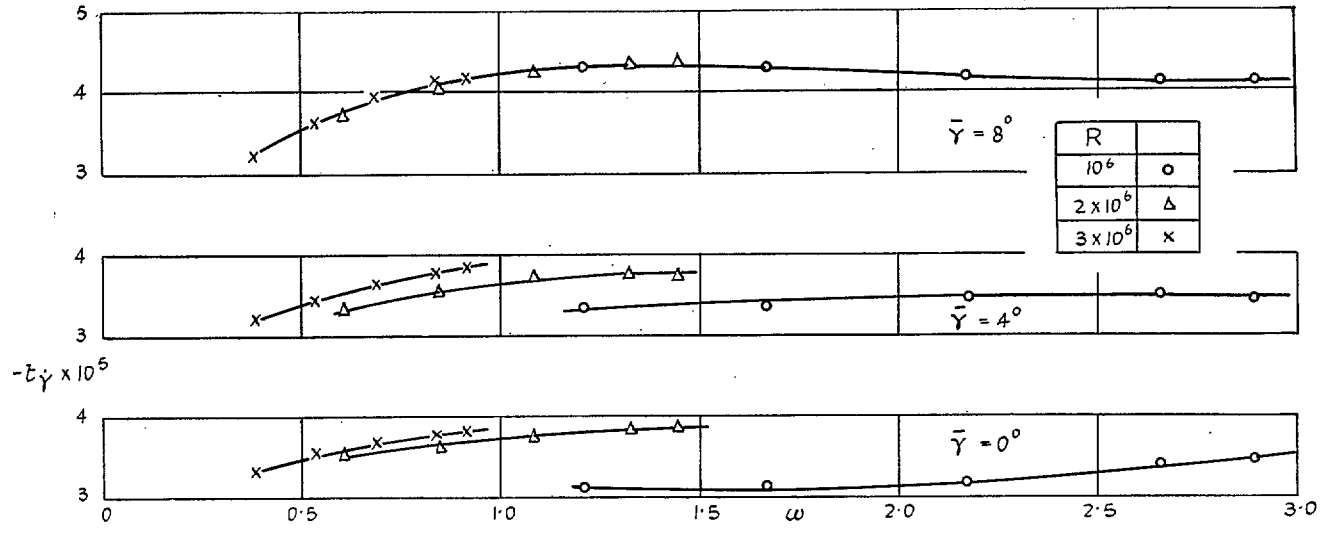

Variation of t_γ with frequency parameter—transition at 0·1c.

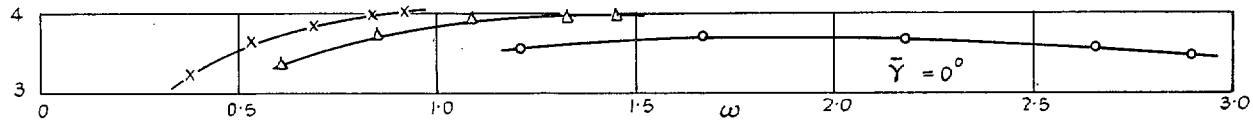

FIG. 4. Variation of t_γ with frequency parameter—transition at 0·4c.

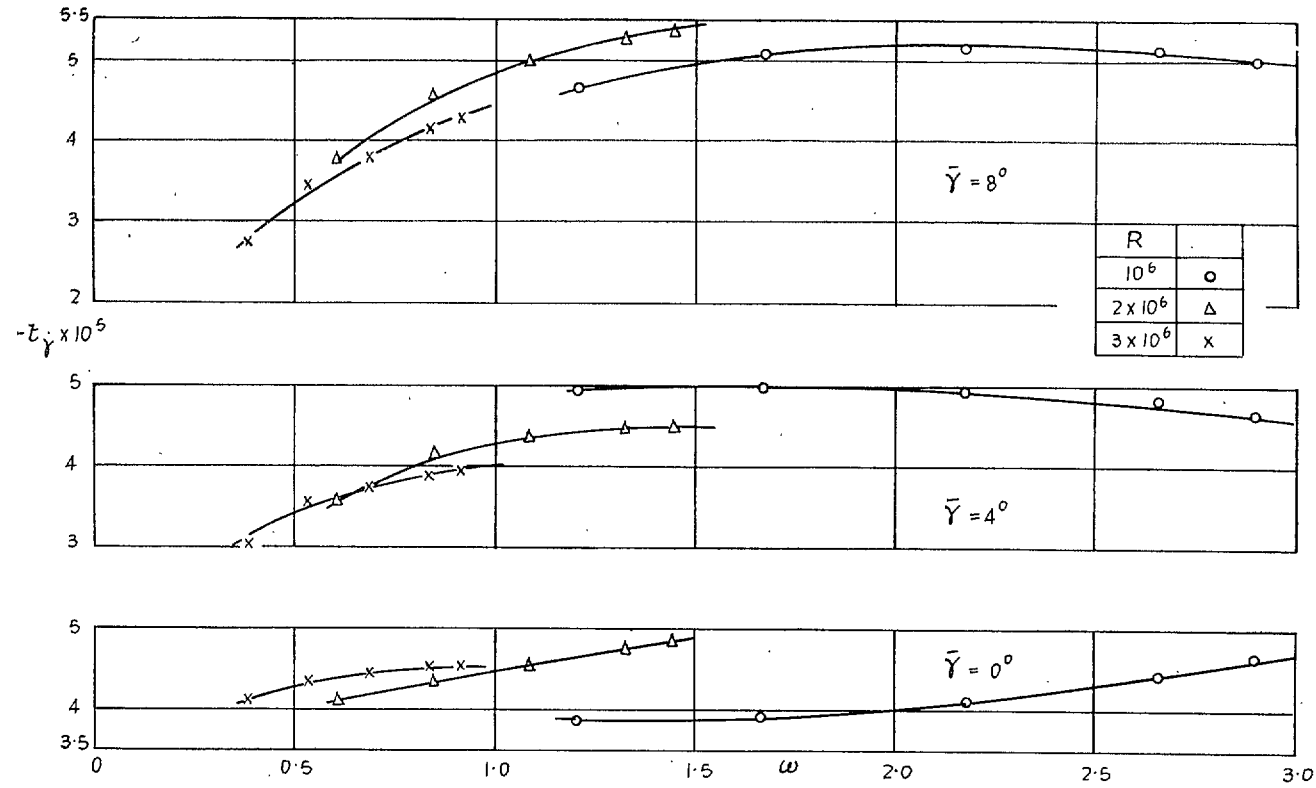

FIG. 5. Variation of l_γ with frequency parameter—natural transition.

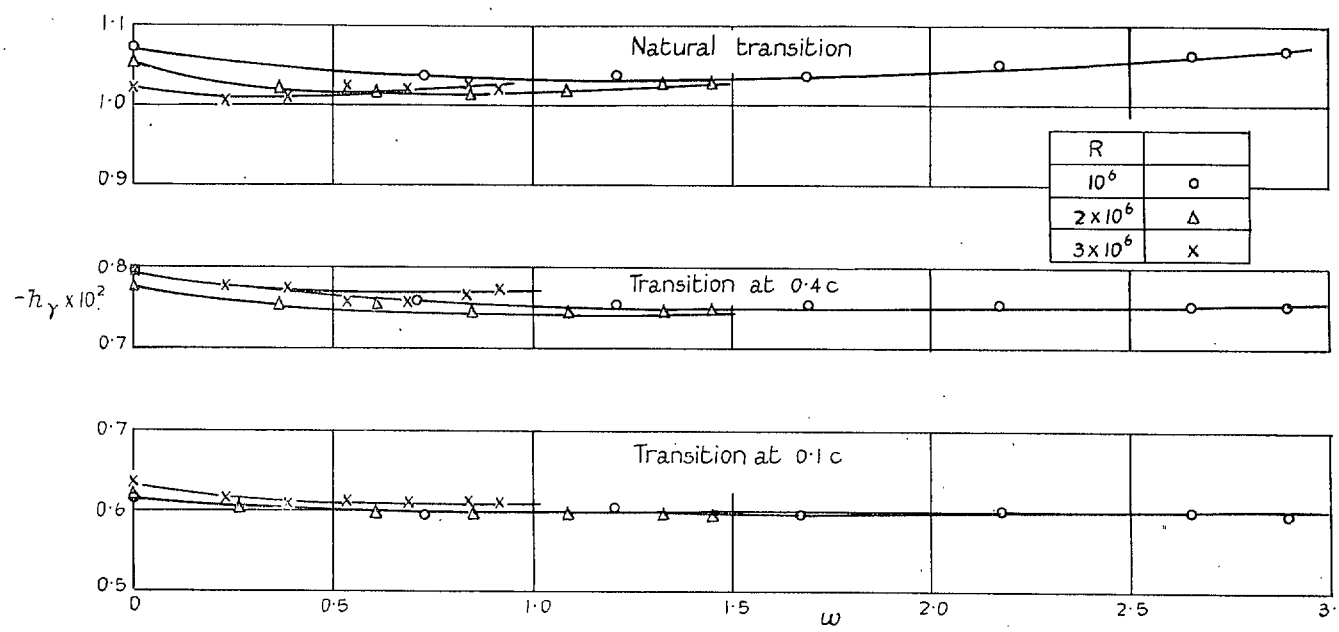

FIG. 6. Variation of h_γ with frequency parameter.

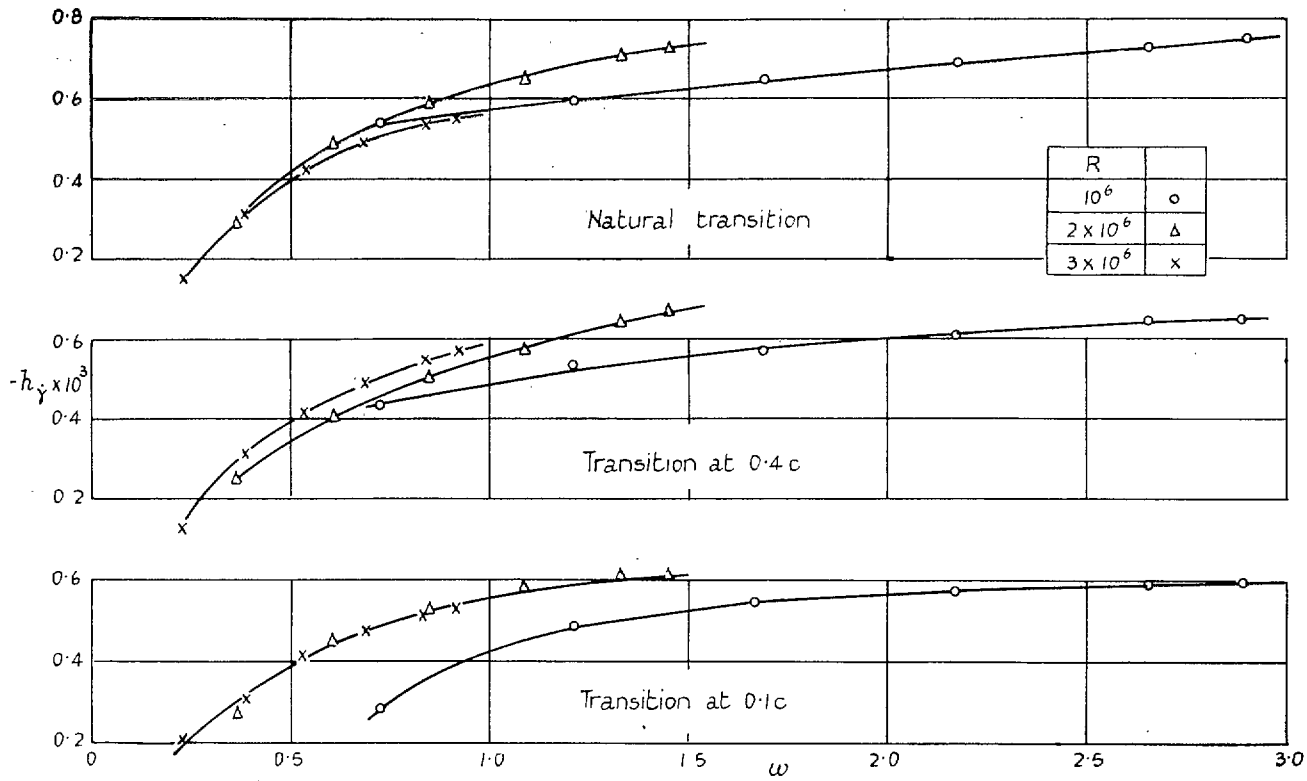

FIG. 7. Variation of h_γ with frequency parameter.

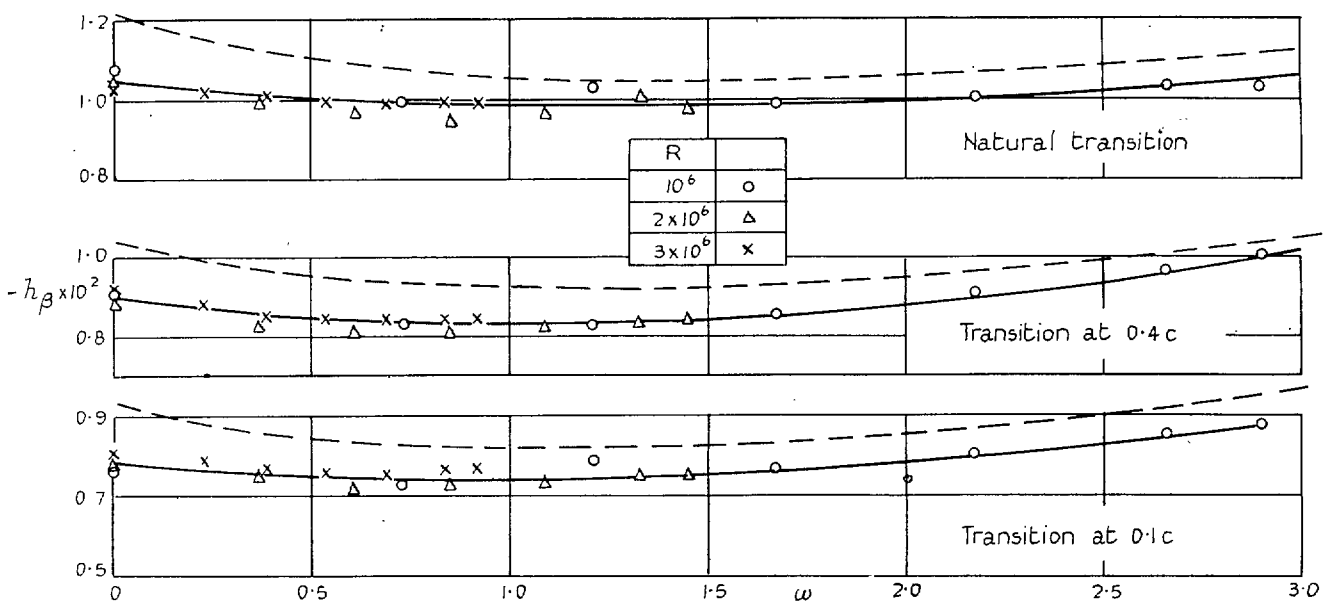

——— 15 deg trailing-edge angle; – – – $12\frac{1}{2}$ deg trailing-edge angle, $R = 10^6$ (ref. 1).

FIG. 8. Variation of h_β with frequency parameter.

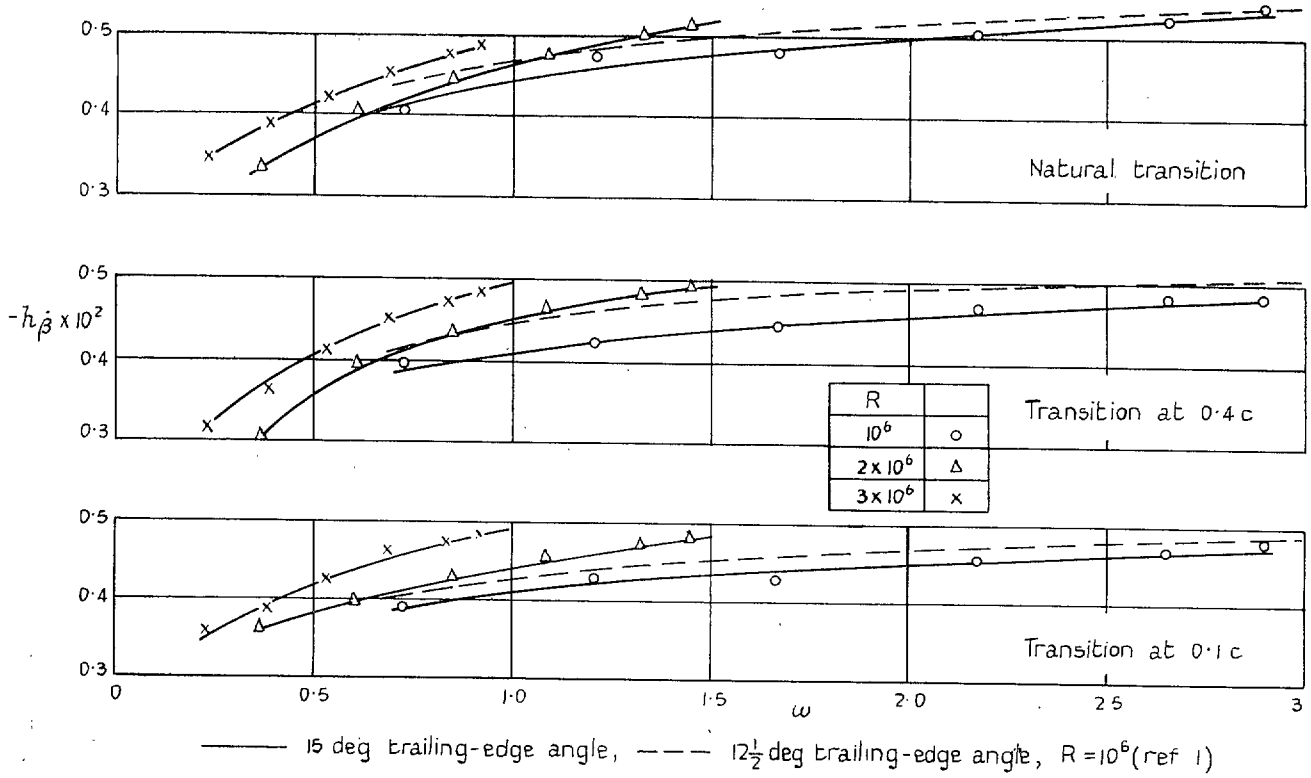

FIG. 9. Variation of $h_{\dot{\beta}}$ with frequency parameter.

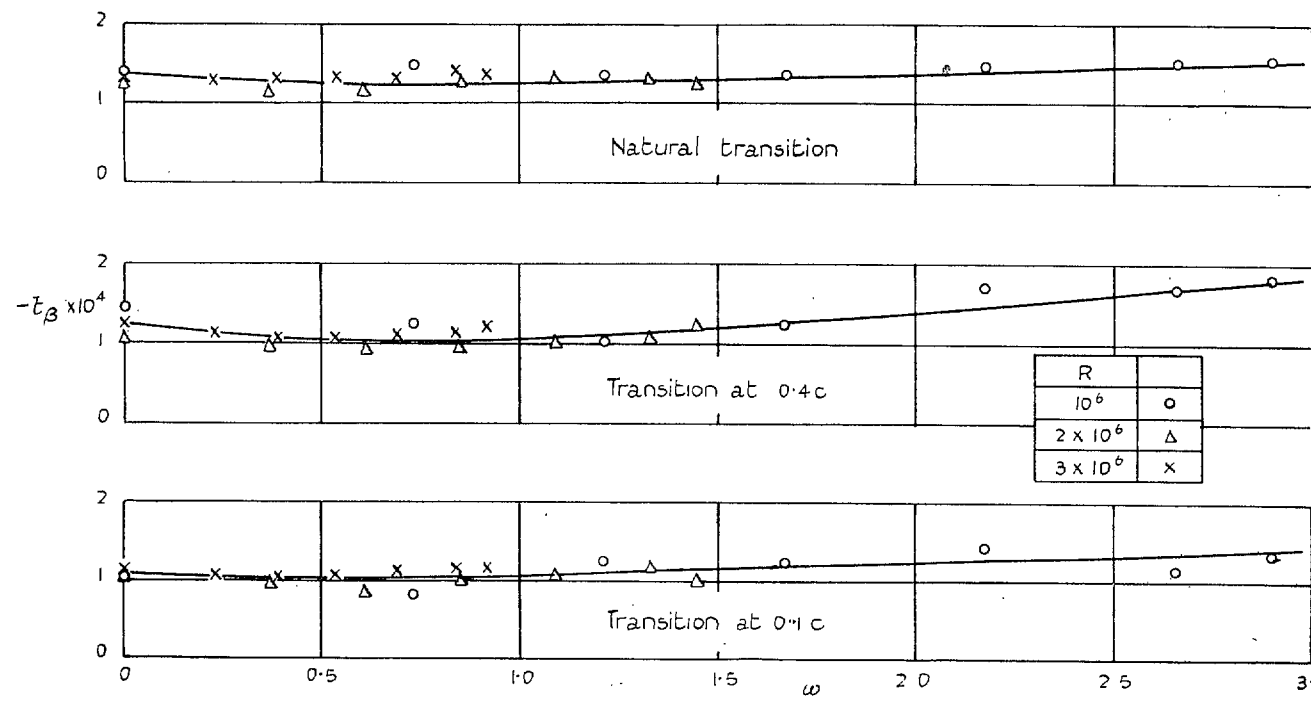

FIG. 10. Variation of $t_{\dot{\beta}}$ with frequency parameter.

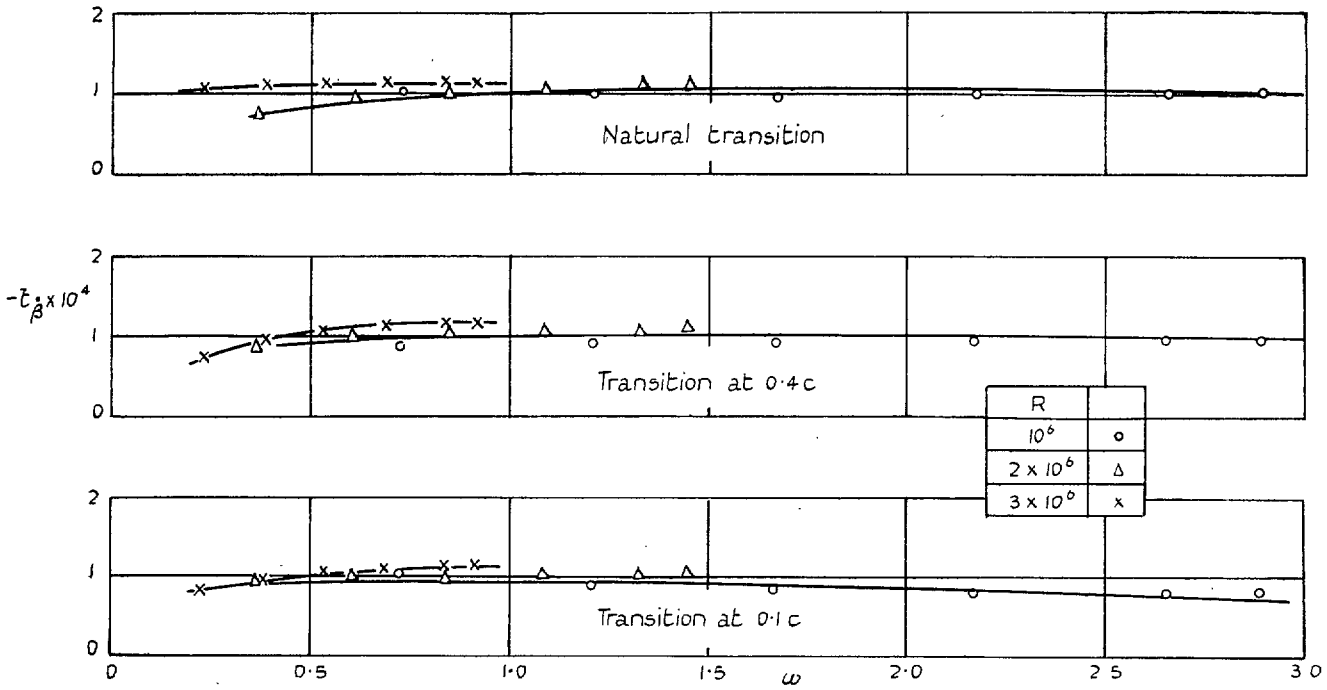

FIG. 11. Variation of t_β with frequency parameter.

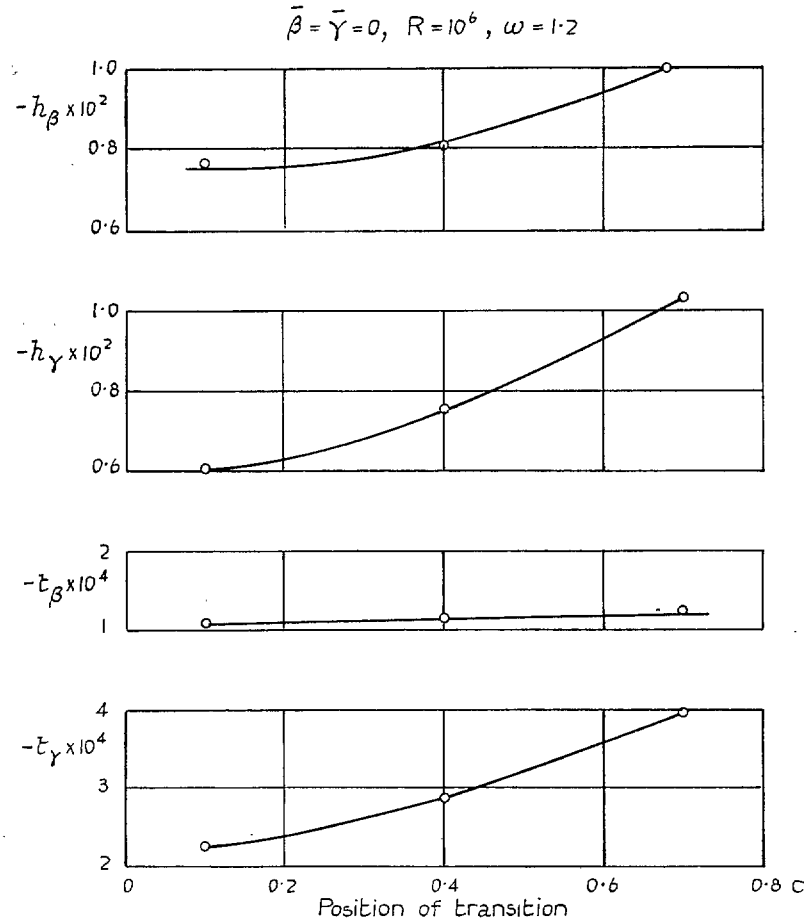

FIG. 12. Variation of h_β, h_γ, t_β, t_γ with transition position.

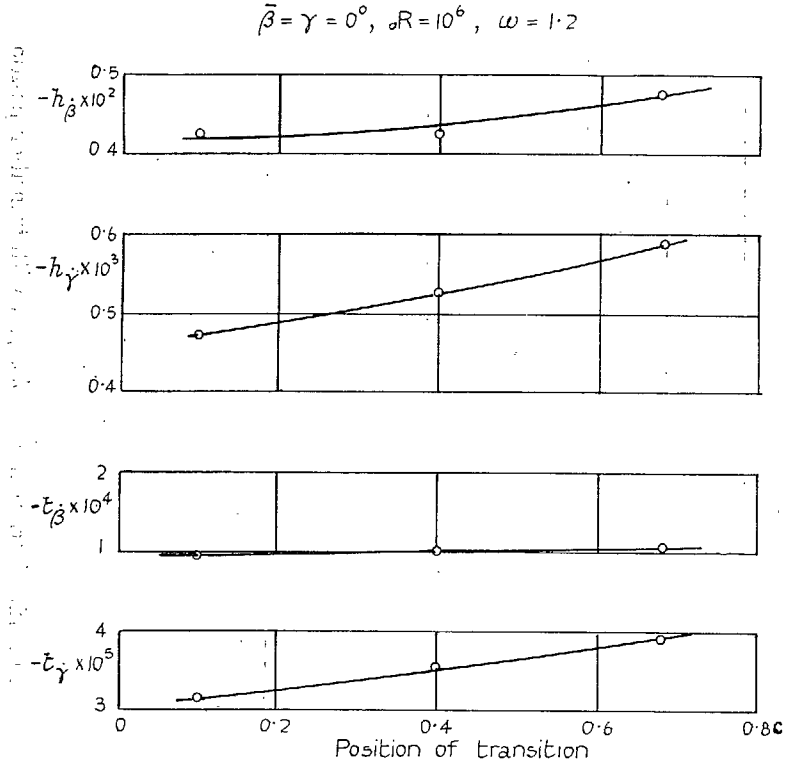

FIG. 13. Variation of $h_{\dot{\beta}}$, $h_{\dot{\gamma}}$, $t_{\dot{\beta}}$, $t_{\dot{\gamma}}$ with transition position.

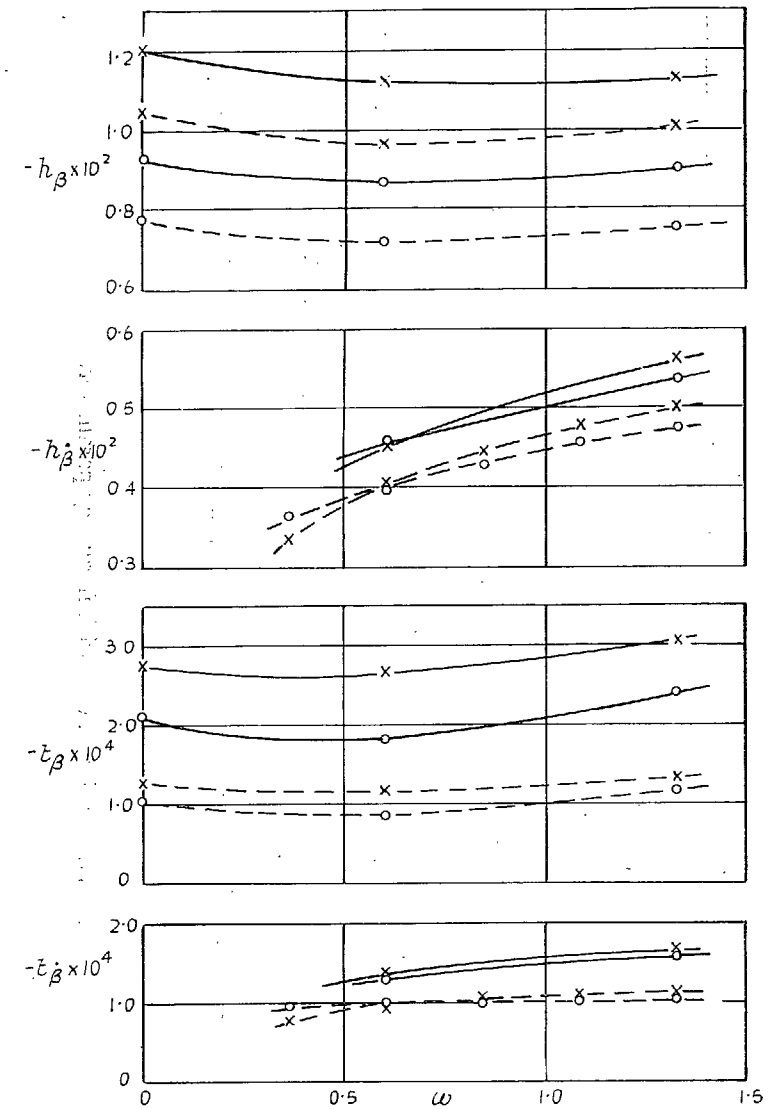

$\bar{\beta} = 0°$, $R = 2 \times 10^6$

o Transition at 0·1c, x Natural transition, —— Tab-gap sealed
– – Tab-gap open

FIG. 14. Effect of gap on h_{β}, $h_{\dot{\beta}}$, t_{β}, $t_{\dot{\beta}}$.

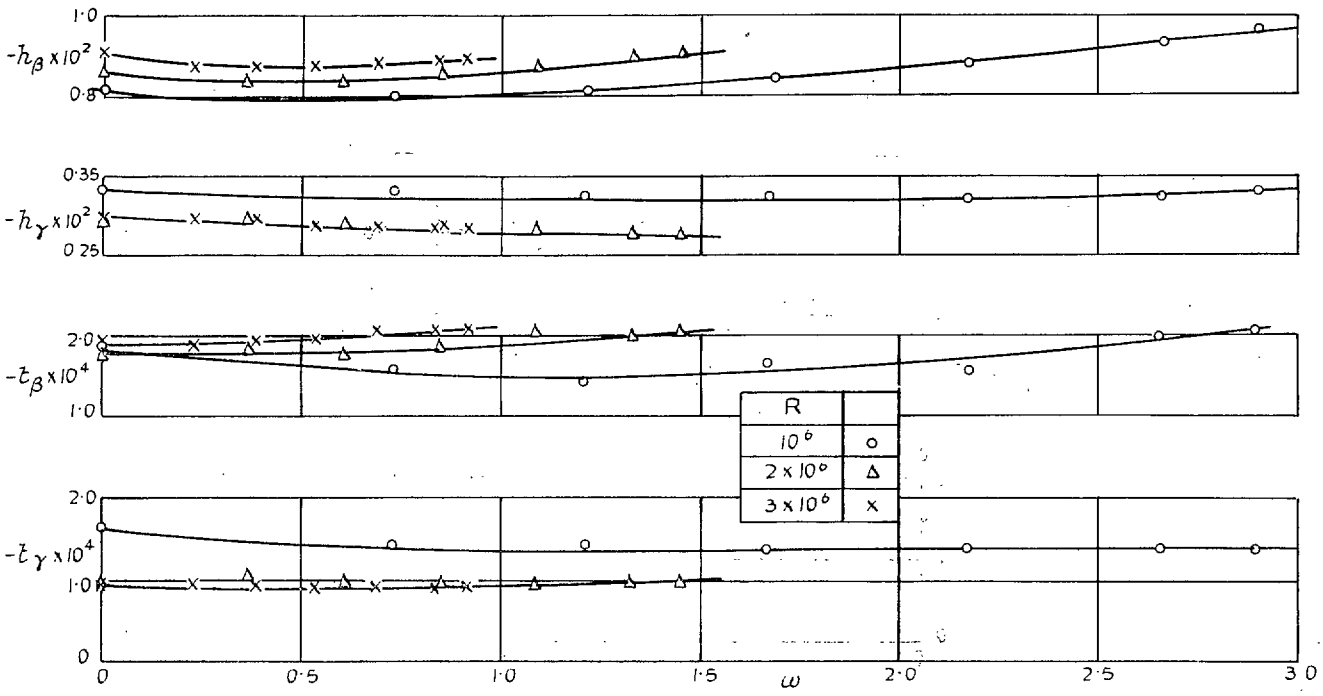

FIG. 15. Variation of h_β, h_γ, t_β, t_γ with frequency parameter.
$\bar{\beta} = -8$ deg, $\bar{\gamma} = +12{\cdot}4$ deg. Transition at $0{\cdot}1c$.

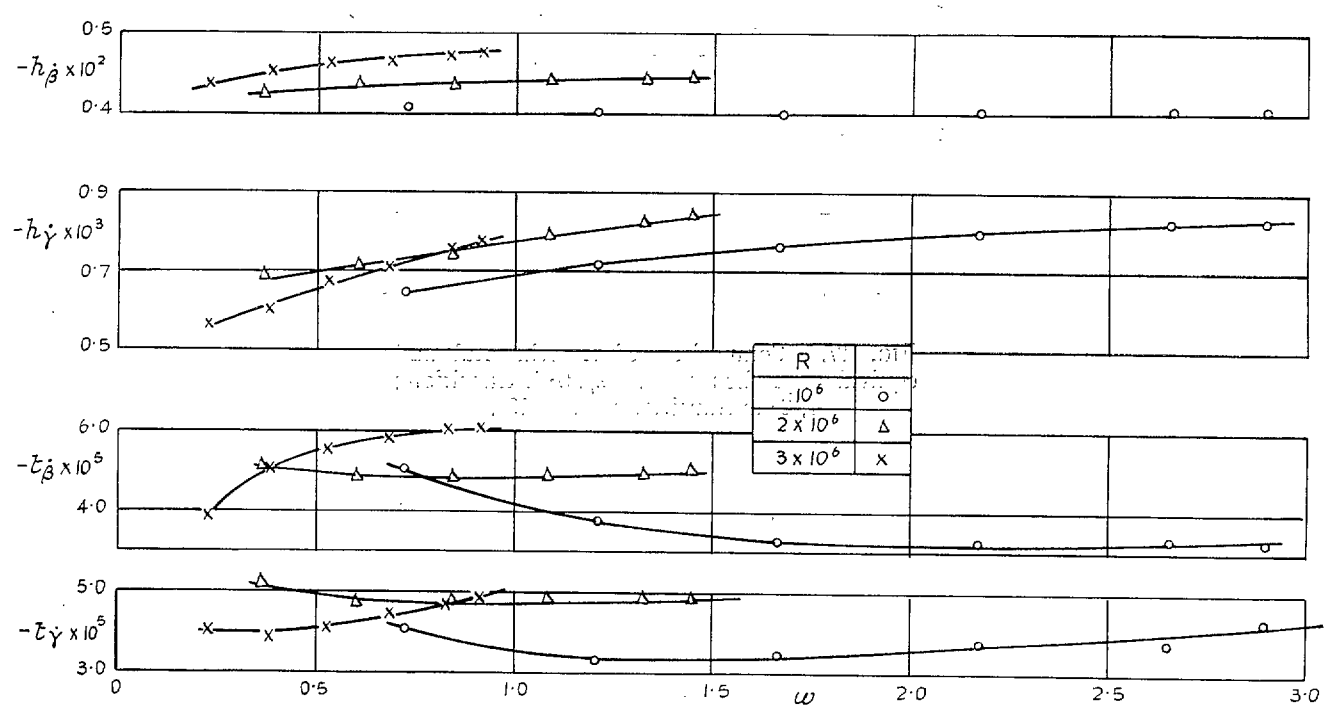

FIG. 16. Variation of h_β, h_γ, t_β, t_γ with frequency parameter.
$\bar{\beta} = -8$ deg, $\bar{\gamma} = +12{\cdot}4$ deg. Transition at $0{\cdot}1c$.

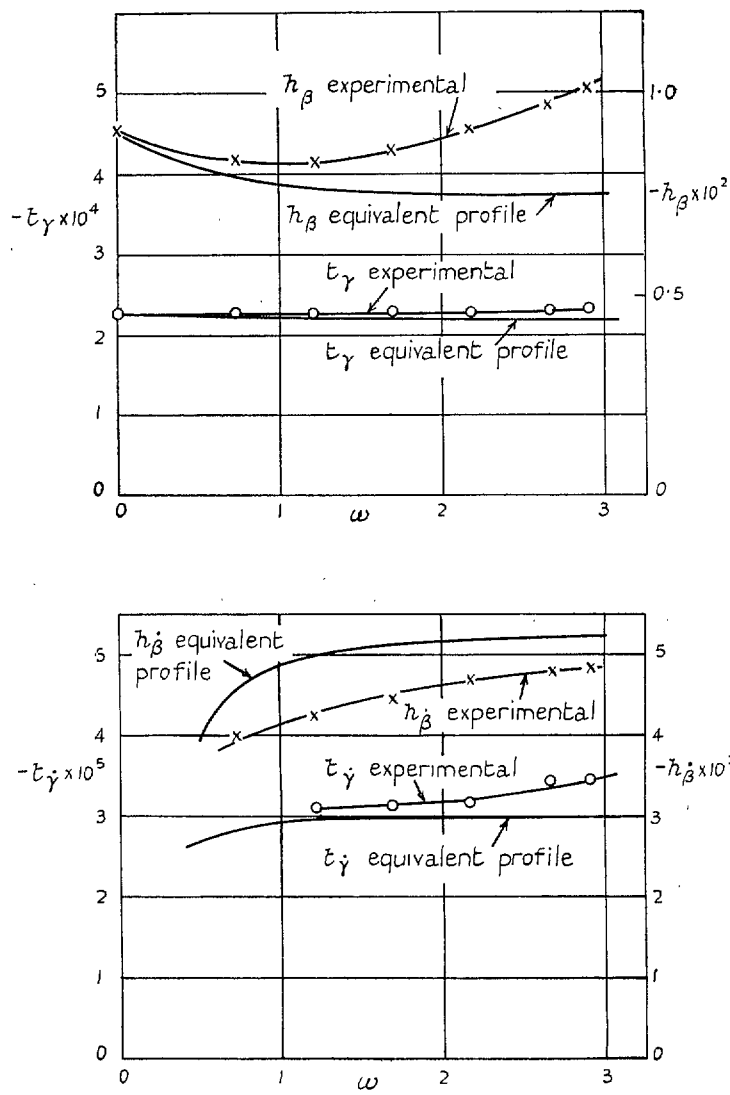

FIG. 17. Comparison of experimental and equivalent profile results. h_β, $0{\cdot}4c$ transition; t_γ, $0{\cdot}1c$ transition; $R = 10^6$.

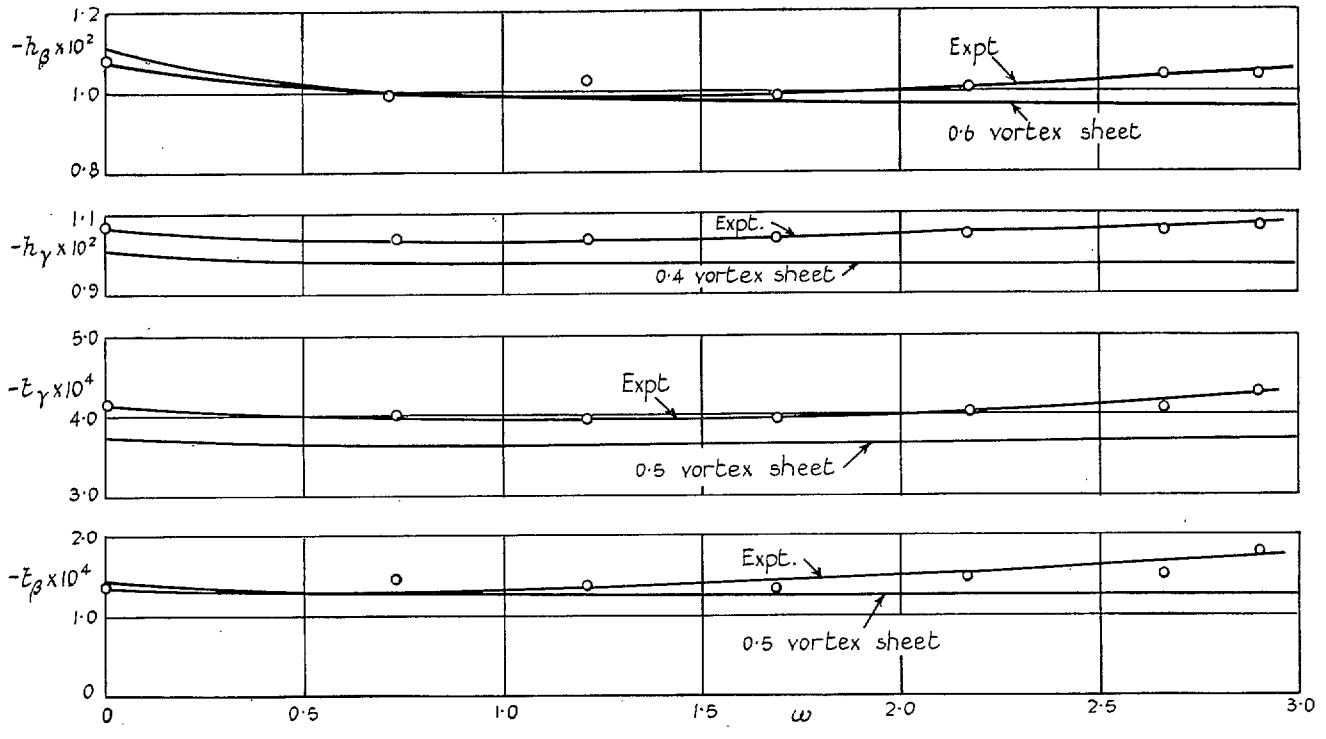

FIG. 18. Comparison of vortex sheet and experimental results.
$\bar{\beta} = \bar{\gamma} = 0$ deg, $R = 10^6$, natural transition, 'o' experimental.

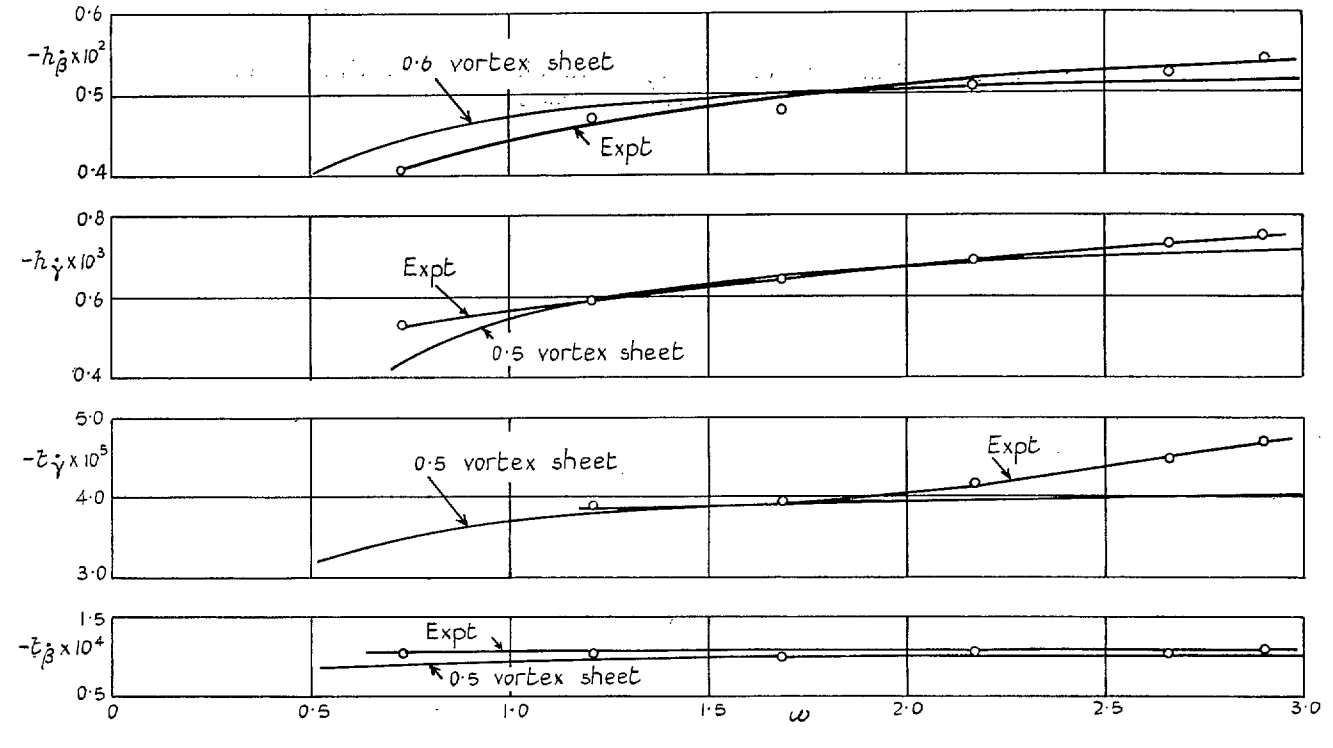

FIG. 19. Comparison of vortex sheet and experimental results.
$\bar{\beta} = \bar{\gamma} = 0$ deg, $R = 10^6$, natural transition, 'o' experimental.

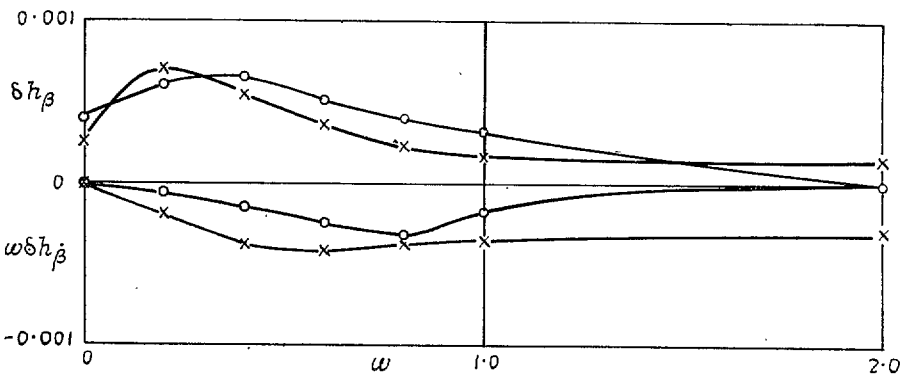

$$\delta h_\beta = h_{\beta\ \text{free stream}} - h_{\beta\ \text{experimental}}$$

$$\omega\delta h_\beta = \omega h_{\dot\beta\ \text{free stream}} - \omega h_{\dot\beta\ \text{experimental}}$$

o Sinnott equivalent profile, $c/h = 0{\cdot}36$
× De Jager, $c/h = 0{\cdot}35$
where h is the distance between tunnel walls

FIG. 20. Comparison of corrections to the direct aileron derivatives for tunnel interference.

(68305) Wt. 20/9036 K.7 1/58 Hw. PRINTED IN GREAT BRITAIN

Publications of the Aeronautical Research Council

ANNUAL TECHNICAL REPORTS OF THE AERONAUTICAL RESEARCH COUNCIL (BOUND VOLUMES)

1939 Vol. I. Aerodynamics General, Performance, Airscrews, Engines. 50*s.* (52*s.*).
Vol. II. Stability and Control, Flutter and Vibration, Instruments, Structures, Seaplanes, etc. 63*s.* (65*s.*)

1940 Aero and Hydrodynamics, Aerofoils, Airscrews, Engines, Flutter, Icing, Stability and Control, Structures, and a miscellaneous section. 50*s.* (52*s.*)

1941 Aero and Hydrodynamics, Aerofoils, Airscrews, Engines, Flutter, Stability and Control, Structures. 63*s.* (65*s.*)

1942 Vol. I. Aero and Hydrodynamics, Aerofoils, Airscrews, Engines. 75*s.* (77*s.*)
Vol. II. Noise, Parachutes, Stability and Control, Structures, Vibration, Wind Tunnels. 47*s.* 6*d.* (49*s.* 6*d.*)

1943 Vol. I. Aerodynamics, Aerofoils, Airscrews. 80*s.* (82*s.*)
Vol. II. Engines, Flutter, Materials, Parachutes, Performance, Stability and Control, Structures. 90*s.* (92*s.* 9*d.*)

1944 Vol. I. Aero and Hydrodynamics, Aerofoils, Aircraft, Airscrews, Controls. 84*s.* (86*s.* 6*d.*)
Vol. II. Flutter and Vibration, Materials, Miscellaneous, Navigation, Parachutes, Performance, Plates and Panels, Stability, Structures, Test Equipment, Wind Tunnels. 84*s.* (86*s.* 6*d.*)

1945 Vol. I. Aero and Hydrodynamics, Aerofoils. 130*s.* (132*s.* 9*d.*)
Vol. II. Aircraft, Airscrews, Controls. 130*s.* (132*s.* 9*d.*)
Vol. III. Flutter and Vibration, Instruments, Miscellaneous, Parachutes, Plates and Panels, Propulsion. 130*s.* (132*s.* 6*d.*)
Vol. IV. Stability, Structures, Wind Tunnels, Wind Tunnel Technique. 130*s.* (132*s.* 6*d.*)

Annual Reports of the Aeronautical Research Council—

1937 2*s.* (2*s.* 2*d.*) 1938 1*s.* 6*d.* (1*s.* 8*d.*) 1939–48 3*s.* (3*s.* 5*d.*)

Index to all Reports and Memoranda published in the Annual Technical Reports, and separately—

April, 1950 - - - - R. & M. 2600 2*s.* 6*d.* (2*s.* 10*d.*)

Author Index to all Reports and Memoranda of the Aeronautical Research Council—

1909—January, 1954 R. & M. No. 2570 15*s.* (15*s.* 8*d.*)

Indexes to the Technical Reports of the Aeronautical Research Council—

December 1, 1936—June 30, 1939	R. & M. No. 1850	1*s.* 3*d.* (1*s.* 5*d.*)
July 1, 1939—June 30, 1945	R. & M. No. 1950	1*s.* (1*s.* 2*d.*)
July 1, 1945—June 30, 1946	R. & M. No. 2050	1*s.* (1*s.* 2*d.*)
July 1, 1946—December 31, 1946	R. & M. No. 2150	1*s.* 3*d.* (1*s.* 5*d.*)
January 1, 1947—June 30, 1947	R. & M. No. 2250	1*s.* 3*d.* (1*s.* 5*d.*)

Published Reports and Memoranda of the Aeronautical Research Council—

Between Nos. 2251–2349	R. & M. No. 2350	1*s.* 9*d.* (1*s.* 11*d.*)
Between Nos. 2351–2449	R. & M. No. 2450	2*s.* (2*s.* 2*d.*)
Between Nos. 2451–2549	R. & M. No. 2550	2*s.* 6*d.* (2*s.* 10*d.*)
Between Nos. 2551–2649	R. & M. No. 2650	2*s.* 6*d.* (2*s.* 10*d.*)
Between Nos. 2651–2749	R. & M. No. 2750	2*s.* 6*d.* (2*s.* 10*d.*)

Prices in brackets include postage

HER MAJESTY'S STATIONERY OFFICE

York House, Kingsway, London W.C.2; 423 Oxford Street, London W.1; 13a Castle Street, Edinburgh 2; 39 King Street, Manchester 2; 2 Edmund Street, Birmingham 3; 109 St. Mary Street, Cardiff; Tower Lane, Bristol 1; 80 Chichester Street, Belfast, *or through any bookseller.*

S.O. Code No. 23–3029